Drosophila Neuronal Glucose 6 Phosphatase is a Modulator of Neuropeptide Release that Regulates Muscle Glycogen Stores via FMRFamide Signaling

Tetsuya Miyamoto, Sheida Hedjazi, Chika Miyamoto and Hubert Amrein
Department of Cell Biology and Genetics
School of Medicine
Texas A&M University
Bryan, Texas

12 **SIGNIFICANCE STATEMENT**
13
14 Glucose-6-phosphtase (G6P) is a critical enzyme in sugar synthesis and catalyzes the final
15 step in glucose production. In *Drosophila* - and insects in general - where trehalose is the
16 circulating sugar and Trehalose phosphate synthase, and not G6P, is used for sugar
17 production, G6P has adopted a novel and unique role in peptidergic neurons in the CNS.
18 Interestingly, flies lacking *G6P* show diminished Neuropeptide secretions and have a smaller
19 Golgi apparatus in peptidergic neurons. It is hypothesized that the role of G6P is to
20 counteract glycolysis, thereby creating a cellular environment that is more amenable to
21 efficient neuropeptide secretion.

SUMMARY

Neuropeptides (NPs) and their cognate receptors are critical effectors of diverse physiological processes and behaviors. We recently reported of a non-canonical function of the *Drosophila Glucose-6-Phosphatase* (*G6P*) gene in a subset of neurosecretory cells in the CNS that governs systemic glucose homeostasis in food deprived flies. Here, we show that *G6P* expressing neurons define 6 groups of neuropeptide secreting cells, 4 in the brain and 2 in the thoracic ganglion. Using the glucose homeostasis phenotype as a screening tool, we find that neurons located in the thoracic ganglion expressing FMRFamide neuropeptides (*FMRFa*^{G6P} neurons) are necessary and sufficient to maintain systemic glucose homeostasis in starved flies. We further show that *G6P* is essential in *FMRFa*^{G6P} neurons for attaining a prominent Golgi apparatus and secreting neuropeptides efficiently. Finally, we establish that *G6P* dependent FMRFa signaling is essential for the build-up of glycogen stores in the jump muscle which expresses the receptor for FMRFamides. We propose a general model in which the main role of *G6P* is to counteract glycolysis in peptidergic neurons for the purpose of optimizing the intracellular environment best suited for the expansion of the Golgi apparatus, boosting release of neuropeptides and enhancing signaling to respective target tissues expressing cognate receptors.

42 **INTRODUCTION**

43

44 Neuropeptides (NPs) play central roles in modulating physiology and behaviors. In
45 humans, more than one hundred NPs have been identified, and most of them act through
46 known G protein coupled receptors expressed in specific neurons of the brain or target cells
47 in non-neuronal organs and tissues (Nässel and Zandawala, 2019; van den Pol, 2012).
48 *Drosophila melanogaster* has become an important model system for investigating the
49 diverse functions of NPs and their receptors, due to the expansive array of molecular genetic
50 tools, the ability to visualize electrophysiological activity and the availability of powerful
51 behavioral assays. More than 40 NP genes have been described in the fruit fly, many of which
52 encode multiple peptides, and for many of these, cognate receptors have been identified
53 (Nässel and Zandawala, 2019). We recently reported expression of the gluconeogenic enzyme
54 Glucose-6-phosphatase (G6P) in small subpopulations of peptidergic neurons in the fly CNS.
55 By expressing a CFP/YFP based glucose sensor, we showed that G6P is functional in these cells
56 for not only maintaining intracellular glucose levels when flies are food deprived, but also as
57 a critically important enzyme necessary for the conversion of alanine to glucose (Miyamoto
58 and Amrein, 2019). At the systemic level, we found that starved *G6P* mutant flies failed to
59 maintain whole body glucose homeostasis, a phenotype that is not only rescued by
60 expression of a *G6P* transgene, but also by activation of *G6P* neurons using the heat-activated
61 channel TRPA1 in *G6P* mutant flies. Taken together, these observations indicated that the role
62 of *G6P* in these neurons is not to produce glucose, but to facilitate peptidergic signaling,
63 disruption of which causes loss of whole-body glucose homeostasis in starved flies.

64 In mammals, G6P is mainly known as a key liver and kidney enzyme during
65 gluconeogenesis and glycogenolysis, metabolic processes upregulated in food-deprived
66 animals. G6P hydrolyses g-6-p to glucose, which is then released into the blood stream to
67 maintain glucose homeostasis. These two pathways are highly conserved across different
68 animal lineages including insects, where they take place in the adipose (fat body) and
69 Malpighian tubules, tissues analogous to the mammalian liver and kidney, respectively.
70 However, the last enzymatic step is distinct in insects, whereby g-6-p is converted to trehalose,
71 the main circulating insect sugar, using the enzyme trehalose 6 phosphate synthase 1 (TPS1)
72 to ensure sugar homeostasis when flies are starved (Matsuda et al., 2015; Thompson, 2003).
73 Thus, the existence of a conserved *Drosophila* G6P enzyme in general, and its expression in

74 peptidergic neurons specifically, which are not known to be involved in systemic sugar
75 homeostasis, raises intriguing questions about its function in NP signaling. First and foremost,
76 what is the neuronal identity of the approximately 30 *G6P-GAL4* expressing neurons in the
77 CNS, beyond the fact that they express DIMMED, a marker for large NP producing neurons
78 (Hewes et al., 2003)? Second, which of these neurons mediate whole body glucose
79 homeostasis in starved flies, the only know function of *G6P* in insects? Third, what is the
80 cellular role of G6P in peptidergic neurons? And fourth, what is the primary systemic
81 phenotype that ultimately leads to failed glucose homeostasis in starved *G6P* mutant flies?
82 In this paper, we provide answers to these questions. We determined the identity of
83 *G6P* neurons in the fly CNS by correlating *G6P-GAL4* expression with the location of NP
84 producing neurons. Specifically, we identified subsets of large neuropeptide F (NPF),
85 Orcokinin A (OrcoA), pigment-dispersing factor (Pdf), FMRFamide and IPNamide - positive
86 neurons that also express *G6P-GAL4.* By inhibiting neural activity and rescuing G6P function
87 in *G6P* mutant flies in each of these subsets, we show that *FMRFa* expressing *G6P* neurons
88 ($FMRFa^{G6P}$) located in the thoracic ganglia alone are necessary and sufficient to maintain
89 whole body glucose homeostasis in food deprived flies. We further narrowed down the
90 precise subset of $FMRFa^{G6P}$ neurons using the split GAL4 system and found that they
91 correspond to four pairs of ventrally located large FMRFa expressing neurons (T1v, T2v and
92 T3v and T2va neurons; Schneider et al., 1993b). Moreover, we have uncovered the first
93 cellular phenotypes associated with $FMRFa^{G6P}$ neurons, namely a smaller Golgi apparatus and
94 reduced NP secretion from $FMRFa^{G6P}$ neurons. Lastly, we describe the primary systemic role
95 mediated by *G6P* and *FMRFa*, by homing in on the FMRFa receptor (FMRFaR). Specifically,
96 we show that *FMRFaR* is expressed in the jump muscle and that muscle glycogen content of
97 $G6P^{-/-}$, $FMRFa^{-/-}$ and $FMRFaR^{-/-}$ flies is reduced by about 50 percent, compared to wild type
98 controls. These observations indicate that FMRFa-FMRFaR signaling is essential to build up
99 glycogen stores under normal feeding conditions, and they suggest that the loss of whole-
100 body glucose homeostasis observed of starved *G6P* mutants is due to the inability of these
101 flies to draw upon stored glycogen. We propose that G6P counteracts glycolysis in NP
102 secreting neurons, thereby establishing a cellular environment that is more amenable to the
103 expansion of the Golgi apparatus and large dense core vesicles, which in turn enhances NP
104 release.
105

106 **RESULTS**

107

108 **Identification of *G6P-GAL4* neuronal subtypes**

109 Initial expression analysis of *G6P-GAL4; UAS-mCD8GFP* flies revealed the presence of
110 approximately 14 GFP positive neurons in the brain (Miyamoto and Amrein, 2019). Three lines
111 of evidence suggested that most, if not all, *G6P* expressing neurons were NP producing cells:
112 First, they are relatively large in appearance and express DIMMED, a transcriptional regulator
113 that plays a key role in cell fate determination of NP producing cells (Hewes et al., 2003).
114 Second, one pair of cells located in the dorsomedial region co-expresses NPF, a *Drosophila*
115 homolog of mammalian NPY. And third, examination of *G6P* expression in the thoracic
116 ganglion showed many additional *G6P* positive cells, in a pattern similar to that described for
117 neurons expressing FMRFamide and IPNamide (Lundquist and Nässel, 1990; Schneider et al.,
118 1993b; Verleyen et al., 2004). These observations suggested that *G6P* is found in diverse
119 populations of peptidergic neurons, expressing different NPs. We therefore set out to
120 determine the identity of these NPs by comparing locations of G6P positive neurons with
121 available reports of NP expression profiles, comprehensively reviewed by Nässel and
122 Zandawala (Nässel and Zandawala, 2019). Based on this comparison, we carried out double
123 staining experiments of brain and thoracic ganglia preparations of *G6P-GAL4*; *UAS-mCD8GFP*
124 flies using NP specific antibodies and identified five NPs co-expressed with *G6P-GAL4* (Figure
125 1). In the brain, in addition to the prominent pair of $G6P^{NPF}$ neurons, Orcokinin-A, PDF and
126 IPNa were found to be expressed in subsets of *G6P-GAL4* neurons (Figure 1A-1E, referred to
127 as $Orco^{G6P}$, PDF^{G6P}, $IPNa^{Br_G6P}$ neurons), while in the thoracic ganglion, a group of FMRFa-
128 positive neurons and a second subset of IPNa-positive neurons co-expressing *G6P-GAL4* were
129 identified (Figure 1G-1I, referred to $FMRFa^{G6P}$ and $IPNa^{Th_G6P}$ neurons; note that the FMRFa-
130 positive neurons present in the brain do not express *G6P-GAL4*; Figure 1F). Neurons
131 expressing a given NP fall generally into two groups: a small number of neurons presenting
132 with large cell bodies, and a larger number of neurons presenting with smaller cell bodies
133 (Figure 1). For example, in the brain, there are some 20 NPF expressing neurons, only four of
134 which fall into the large size class (Shao et al., 2017) (Figure 1J). Likewise, only two of the 10
135 Orcokinin positive neurons fall into the large class, while about half of the PDF positive
136 neurons correspond to the large ventral lateral clock neurons (large LN-Vs) (Taghert et al.,
137 2001). Of note, G6P is only expressed in large neurons, both in the brain and the thoracic

138 ganglion (Figure 1B-1E, 1H and 1I). Together, about 30 of the 60 large neurons expressing the
139 five NPs are G6P-positive (*NP*^{G6P} neurons).
140 In order to functionally manipulate subpopulations of specific NP expressing neurons,
141 we procured *GAL4* lines expressed in Orcokinin, IPNa and FMRFa producing neurons from
142 the *Flylight* repository (https://www.janelia.org/project-team/flylight) or obtained previously
143 characterized lines for NPF (Wu et al., 2003) and PDF (Renn et al., 1999), respectively. We
144 confirmed *GAL4* expression with these NPs by co-immunostaining brains and thoracic ganglia
145 of *NP-GAL4; UAS-mCD8GFP* flies (Supplementary Figure 1).
146
147 **FMRFa peptides mediate glucose homeostasis**
148 Expression of *G6P* in different NP secreting neurons suggests that G6P activity impacts
149 several distinct NP signaling pathways. Using *G6P* mutant flies, we previously showed that
150 one function of this enzyme is to maintain whole-body glucose homeostasis in starved flies,
151 while having no significant impact on the levels of trehalose. Importantly, whole-body glucose
152 homeostasis can be complemented in *G6P* mutant flies by temperature induced neural
153 activation of *G6P* neurons (Miyamoto and Amrein, 2019) using *UAS-TRPA1* (Parisky et al.,
154 2008). Similarly, silencing all *G6P-GAL4* expressing neurons using *UAS-Kir2.1* encoding the
155 inward rectifier potassium channel Kir2.1 (Baines et al., 2001; Paradis et al., 2001) mimicked
156 the whole-body glucose homeostasis phenotype of *G6P* mutant flies (Figure 2A)(Miyamoto
157 and Amrein, 2019). To determine which subset of *NP*^{G6P} neurons is responsible for glucose
158 homeostasis, we expressed *UAS-Kir2.1* under the control of the five NP specific *GAL4* drivers.
159 Inactivation of *NPF*^{G6P}, *Orco*^{G6P}, *PDF*^{G6P}, *IPNa*^{Br_G6P} or *IPNa*^{TG_G6P} neurons caused no change in
160 whole body glucose levels under either fed or starved conditions (Figure 2A). Only expression
161 of *UAS-Kir2.1* in *FMRFa*^{G6P} neurons (*GMR18C05-GAL4*) led to significantly reduced glucose
162 levels in starved flies (Figure 2A). Consistent with our previous analysis, trehalose levels were
163 not significantly different when compared to wild type control flies (Supplementary Figure 2).
164 To test whether the function of *G6P* in *FMRFa* positive neurons is sufficient for maintaining
165 whole body glucose homeostasis, we measured glucose levels in *G6P* mutant flies expressing
166 a *UAS-G6P* transgene under the control of *GMR18C05-GAL4*. Indeed, these flies showed fully
167 restored whole body glucose levels under starving conditions (Figure 2B). Taken together,
168 these experiments identified *FMRFa*^{G6P} neurons in the thoracic ganglion as the neurons
169 responsible for maintaining whole body glucose homeostasis in food deprived flies.

170 *G6P-GAL4* exhibits varied expression in the thoracic ganglion. While consistently
171 observed in three to four cells in the meso-thoracic segment, expression varied in the pro-
172 and metathoracic segments. Thus, we sought to investigate overlap between *G6P* and *FMRFa*
173 in more detail using the split GAL4 system, which reveals expression of a reporter only in cells
174 that co-express two independent drivers controlled by the promotors of two genes of interest
175 (Luan et al., 2006; Pfeiffer et al., 2010). We generated split-GAL4 transgenic flies (*G6P-*
176 *GAL4DBD* and a *FMRFa-p65AD*) that also contained a *10xUAS-mCD8GFP* reporter and
177 performed immunostaining of the CNS (Figure 3A and 3D). These experiments revealed that
178 the thoracic ganglion harbored eight large, ventrally located $FMRFa^{G6P}$ neurons, which
179 correspond to four pairs of Tv neurons (T1v, T2v, T2va and T3v; Figure 3A and 3C)(Schneider
180 et al., 1993b). The same eight neurons are also labelled by *GMR18C05-GAL4* (Figure 3B and
181 3C), which we used for the functional characterization of $FMRFa^{G6P}$ neurons in all subsequent
182 experiments (see below). In the brain, the split-GAL4 system and *GMR18C05-GAL4* did not
183 label any FMRFa positive neurons (Figure 3D and 3E), confirming the observations obtained
184 from double staining experiments using *G6P-GAL4* (Figure 1F).
185 *FMRFa* encodes a 347 amino acid long propeptide, which is processed into 14 peptides,
186 10 of which are characterized by the carboxyterminal FMRF motif (Figure 2C) (Predel et al.,
187 2004). To further confirm that FMRFamides are the signaling molecules mediating glucose
188 homeostasis in starved flies, we measured glucose levels in $FMRFa^{P}$ mutant flies. $FMRFa^{P}$ is a
189 P-element insertion into the 11th of the 14 peptides and homozygous $FMRFa^{P}$ mutant, starved
190 flies showed the same glucose homeostasis deficit as flies in which these neurons were
191 silenced (Figure 2D). We also generated a CRISPR/Cas-9 null allele, a deletion encompassing
192 all 14 peptides (*ΔFMRFa*, Figure 2C, Supplementary Figure 3), and found that *ΔFMRFa* flies
193 showed reduced whole body glucose levels in both fed and starved conditions (Figure 2D).
194
195 **G6P is necessary to maintain glucose levels in $FMRFa^{G6P}$ neurons**
196 NPF^{G6P} neurons in the brain require G6P cell-autonomously to maintain intracellular
197 glucose levels when flies are starved (Miyamoto and Amrein, 2019). In these experiments,
198 we employed the fluorescent sensitive glucose sensor Glu700 and found that NPF^{G6P} neurons
199 of starved *G6P* mutant flies were unable to maintain intracellular glucose levels (Miyamoto
200 and Amrein, 2019). While the relevance of this phenomenon for proper neuropeptide
201 signaling remains to be determined, the glucose sensor provides a means to assess whether

202 G6P is also necessary for maintaining intracellular glucose levels in *FMRFa*^{G6P} neurons during
203 starvation. Thus, we established an *in vivo* preparation of the ventral nerve cord that allowed
204 us to monitor glucose levels in these neurons (see Material and Methods). Since G6P is an
205 Endoplasmic Reticulum (ER) resident enzyme (van Schaftingen and Gerin, 2002), we
206 expressed an ER resident version of *Glu700, Glu700KDEL* (Addgene, #17867) under the
207 control of *GMR18C05-GAL4*. In fed *G6P* mutant flies, glucose levels were indistinguishable
208 from wild type fed flies, while in starved flies, *G6P* mutants showed significantly lower glucose
209 levels in *FMRFa*^{G6P} neurons compared to fed flies (Figure 4). Together, these results show that
210 in starved flies, G6P is also functional in *FMRFa*^{G6P} neurons where it maintains intracellular
211 glucose levels during starvation.

212

213 **G6P increases Golgi network volume and facilitates NP release**

214 NP processing involves propeptide cleavage and transport through the Golgi network,
215 ultimately leading to NP deposition in Large Dense Core Vesicles (LDCVs) that derive from the
216 trans Golgi stack (van den Pol, 2012). Thus, we examined whether any difference in size and
217 overall distribution of the ER and Golgi network of *FMRFa*^{G6P} neurons was apparent between
218 *wild type* and *G6P* mutant flies using ER (GFP-KDEL)(Kneen et al., 1998) and Golgi (αManII-
219 GFP) resident reporter proteins (Hardt et al., 2005; Zhou et al., 2014). No obvious differences
220 were observed in the ER. However, the Golgi network occupied a significantly smaller area in
221 *G6P* mutant flies compared to *wild type* flies (Figure 5A 9% vs 14%; see also Supplementary
222 Figure 4). A similar reduction in Golgi volume was also observed when these reporters were
223 expressed in the pair of *NPF*^{G6P}neurons (9% vs 16%, Figure 5B; left panels). Of note, and in
224 contrast to mammalian cells where the Golgi complex is organized as a single ribbon, the
225 *Drosophila* Golgi apparatus is dispersed throughout the cytoplasm (Kondylis and Rabouille,
226 2009).

227 Because LDCVs emerge from the trans Golgi network, NP secretion might be
228 negatively affected in *G6P* mutant flies. To measure the effect of G6P on NP release, we took
229 advantage of the fact that the *FMFRa*^{G6P} neurons correspond to the Tv neurons. These
230 neurons innervate the neurohemal like area in the dorsal neural sheet of the thoracic
231 ganglion, which are release sites into the hemolymph (Lundquist and Nässel, 1990; Schneider

232 et al., 1993b). Thus, NP release from *FMRFa*^{G6P} neurons can be assessed by measuring the NP
233 amounts in the hemolymph. Because available antibodies against FMRFa cross-react with
234 other hemolymph components/peptides, we used the mammalian Atrial natriuretic peptide
235 (Anf) fused to GFP as a proxy NP (Anf-GFP, Husain and Ewer, 2004) and assessed Anf-GFP
236 amounts released into the hemolymph from *FMRFa*^{G6P} neurons of *wild-type* and *G6P* mutant
237 flies, as well as the total amount of Anf-GFP in these flies (Figure 6A and 6B). It was previously
238 established that Anf-GFP is released in a time-appropriate fashion during molting, following
239 the dynamic profile of the resident peptides in these cell, Ecdysis Triggering Hormone (Husain
240 and Ewer, 2004). We expressed the *UAS-Anf-GFP* reporter gene in *FMFRa*^{G6P} neurons and
241 measured peptide levels in the hemolymph. Compared to the *wild-type*, *G6P* mutant flies
242 secrete significantly lower amounts of Anf-GFP into the hemolymph in both fed and starved
243 flies (Figure 6A). Importantly, the deficit can be rescued by inclusion of a *UAS-G6P* transgene.
244 Total amount of Anf-GFP was not affected by *G6P* or lack thereof, but starved flies contained
245 about 30% more NP compared to fed flies (Figure 6B). To explore whether *G6P* dependence
246 can be imposed on non-*G6P* neurosecretory cells, we measured hemolymph and total levels
247 of an epitope tagged, Insulin like peptide 2 (Ilp2), expressed from a genetically modified *Ilp2*
248 gene (*Ilp2*^{1} *gd2HF*) (Park et al., 2014). When *UAS-G6P* was expressed in insulin producing cells
249 (IPCs; *Ilp2*^{1} *gd2HF/dilp2-GAL4 UAS-G6P*), a significant increase of secreted Ilp2HF was
250 observed in starved flies, with a concomitant decrease in total Ilp2HF (Figure 6C and 6D; white
251 bars). Given that IPCs of starved flies do not actively secrete Ilp2HF (Park et al., 2014), this
252 observation implies that ectopic expression of *G6P* triggers quiescent IPCs to secrete Ilp2HF.
253 Total amount of Ilp2HF in fed flies was slightly increased in the presence of G6P, which
254 however, did not result in an increase in secreted Ilp2HF (Figure 6C and 6D; black bars).
255 Furthermore, fed and starved control flies (i.e. flies not expressing G6P) exhibited similar
256 levels of hemolymph Ilp2HF (Figure 6C), an observation that appears counterintuitive based
257 on observations made by Park and colleagues, who reported that hemolymph Ilp2HF spikes
258 rapidly after a meal given to previously starved flies. However, this spike is transient and
259 recedes to levels of starved flies within 60 minutes. (Park et al., 2014). In our experimental
260 set up, fed flies have constant access to food, allowing for a wide range of different feeding
261 states within the cohort at the time of hemolymph collection. Thus, similar amounts of
262 hemolymph Ilp2HF in fed and starved control flies is probably due to the fact only a small
263 fraction of flies, if any, have taken a meal prior to hemolymph collection. Regardless, the

264 observations made in starved flies argues that ectopic expression of *G6P* in IPCs enhances
265 their capabilities to secrete Ilp2HF.
266
267 ***G6P* mediated FMRFa signaling to the jump muscle for glycogen storage**
268 In invertebrates, FMRFamides have been associated with the modulation of heart rate,
269 gut motility, sleep, flight and reproduction (Brussaard et al., 1988; Fisher et al., 1993; Lenz et
270 al., 2015; Nässel and Zandawala, 2019; Ravi et al., 2018). Yet, the roles of FMRFamides and
271 their receptors remains incomplete, in part because many of these studies have been
272 conducted in systems not amenable to molecular genetic analyses. Thus, we sought to
273 determine the target tissue of FMRFamides, expected to express its receptor (FMRFaR,
274 CG2114), and to identify phenotype(s) in flies carrying *FMRFaR* mutations. We took
275 advantage of the chemoconnectomics resource generated by Deng and colleagues, who
276 engineered a series of *GAL4* knock-in lines for many NP receptor genes, including *FMRFaR*
277 (Deng et al., 2019). In adult flies, $FMRFaR^{2A\text{-}GAL4}$ is strongly expressed in the jump muscle and
278 the CNS, while no expression was found in other tissues (flight muscle, reproductive system,
279 fat body, gut etc; Figure 7A), a finding consistent with expression profiles reported in the aging
280 fly cell atlas (Lu et al., 2023). We acquired a *FMRFaR* mutant strain ($FMRFaR^{MB04659}$) and
281 examined the amount of muscle glucose and glycogen in *wild type* and homozygous receptor
282 mutant flies (Figure 7B). While free glucose levels were not noticeably different in the jump
283 muscle, regardless of feeding status, muscle glycogen was significantly lower in fed
284 $FMRFaR^{MB04659}$ homozygous mutant flies, when compared to fed wild type flies (Figure 7B).
285 $FMRFaR^{MB04659}$ mutant flies, regardless of feeding status, exhibited similar glycogen levels as
286 starved wild type flies, which amounts to about 50 percent of that observed in fed wild type
287 flies. Glycogen loss was fully rescued in the presence of a *UAS-FMRFaR* transgene driven by
288 *Act79B-GAL4* (Figure 7C), which is predominantly expressed in the jump muscle (Bryantsev et
289 al., 2012). Importantly, the presence of *ELAV-GAL80* in these flies eliminates the potentially
290 confounding contribution of low level *Act79B-GAL4* expression in the CNS. Moreover, ectopic
291 expression of *FMRFaR* in the fat body, in contrast to expression in the jump muscle, does not
292 restore glycogen levels in *FMRFaR* mutant flies (Figure 7C). And lastly, we note that glycogen
293 levels were also significantly reduced in fed *G6P* and *FMRFa* mutant flies (Figure 7D). Taken
294 together, these results indicate that one key function of FMRFa signaling is the generation of

295 glycogen stores in the jump muscle, which can be accessed to generate glucose in times of
296 limited nutrient availability.
297
298 **DISCUSSION**
299
300 Activity of NPs depends on many external and internal factors, providing a means for
301 temporally and quantitatively controlled release that accommodates an animal's
302 physiological demands. In addition to regulation of transcription and RNA processing
303 (Gauthier and Hewes, 2006; Herzog et al., 1997; Higuchi et al., 2005; Schneider et al., 1993a),
304 most NPs undergo post-translational modification through proteolytic cleavage from
305 precursor proteins (pro-peptides)(Hook et al., 2008; Kovac et al., 2009; Pauls et al., 2014;
306 Rholam and Fahy, 2009). Generally, these regulatory processes are specific to NPs, as they
307 must be tailored to sequence and/or structural features within the specific NP gene or protein.
308 The studies presented here report on a new mode of regulation in NP signaling, namely one
309 that allows modulation across distinct types of secretory neurons expressing the
310 gluconeogenic enzyme G6P. Based on measurements of hemolymph Anf-GFP peptide
311 released from *FMRFa*^{G6P}neurons and Ilp2HF secreted by IPCs ectopically expressing a *UAS-*
312 *G6P* transgene, we postulate that G6P primes peptidergic neurons for more efficient NP
313 release, regardless of the NP they express. Thus, it will be interesting to explore whether G6P
314 modulates NP release in other *NP*^{G6P} neurons and affects respective physiological processes
315 and behaviors, such as courtship (NPF; Liu et al., 2019; Silva et al., 2021), oogenesis (Orcokinin,
316 Silva et al., 2021), circadian behavior and sleep (PDF, Chung et al., 2017; Lear et al., 2009;
317 Parisky et al., 2008), or feeding (NPF, Landayan et al., 2021; Lear et al., 2009; Lee et al., 2004).
318 To our knowledge, a function for an enzyme with an established role in gluconeogenesis and
319 glycogenolysis in neurosecretion, or neurons in general, is unprecedented. While a specific
320 mechanism by which G6P modulates peptidergic neurons remains to be determined, the
321 diminished Golgi size in mutant flies implies that G6P activity creates a cellular environment
322 that is beneficial to Golgi expansion (see below).
323
324 **G6P increases Golgi apparatus and enhances NP release**
325 The central function of mammalian G6P is to catalyze hydrolysis of g-6-p during
326 glycogenolysis or gluconeogenesis, generating free glucose that is exported and released into

327 the blood for systemic glucose homeostasis when animals are food deprived. Despite the fact
328 that *Drosophila* G6P has such catalytic activity in peptidergic neurons and is required to
329 maintain systemic whole-body glucose levels (Miyamoto and Amrein, 2019), multiple lines of
330 evidence argue against a role for *Drosophila* G6P to produce glucose for systemic sugar
331 homeostasis. First, we have previously shown that glucose homeostasis can be restored in
332 starved *G6P* mutant flies by expression of TRPA1 in *G6P* neurons, arguing for a signaling role
333 (Miyamoto and Amrein, 2019). Second, neurons in general have high energy demands and
334 are ill equipped for the generation of glucose, for which major amounts of stored glycogen or
335 incidental supply of amino acids is required. Third and related to this point, while *G6P*
336 peptidergic neurons are diverse, their primary purpose is to produce and secrete NPs, an
337 energy costly process that seems difficult to reconcile with other energy consuming activities
338 such glycogenolysis or gluconeogenesis, although fat cells, which carry out both
339 glycogenolysis and trehaloneogenesis are also prolific hormone producers. And lastly, in
340 nutrient deprived flies, the fat body is well equipped to maintain sugar homeostasis by
341 generating trehalose from g-6-p. These observations, and the fact that neuronal glycolysis is
342 largely dispensable (see below), lead us to posit that the function of *G6P* is to counteract
343 glycolysis in peptidergic neurons, creating conditions that are overall beneficial to the main
344 task of these neurons, the release of NPs.

345 Volkenhoff and colleagues showed that glycolysis is dispensable in neurons
346 (Volkenhoff et al., 2015). Specifically, pan-neuronal RNAi knock down of numerous glycolytic
347 enzymes in the CNS had no impact on survival and overall locomotion, while ubiquitous or
348 pan-glial knock-down of the same genes led to lethality or severe locomotion deficits. Thus,
349 glial but not neuronal glycolysis is essential in the CNS for survival. Moreover, this study also
350 established that lactate generated in glia is shuttled to neurons, where it is used for ATP
351 production via the TCA cycle. While neurons are likely equipped with glycolytic enzymes
352 necessary for energy production, it is apparent that at least in *Drosophila*, neurons rely mostly
353 on metabolites from glia that drive alternative metabolic processes. Based on these findings
354 and the observations reported in this paper, we posit that inhibition of glycolysis in NP^{G6P}
355 neurons creates a cellular environment that enhances production, transport and/or secretion
356 of NPs. For example, shutdown of glycolysis reduces the amounts of glycolytic metabolites,
357 which will affect the intracellular pH and hence might increase efficacy of numerous

358 biochemical processes beneficial for the expansion of the Golgi apparatus and ultimately for
359 NP transport and/or secretion.
360
361 **Diverse roles for G6P enzymes**
362 Humans and most mammals have two additional genes encoding G6P, *G6PC2*
363 expressed in the pancreas, Müller glia cells and spermatids, and the ubiquitously expressed
364 *G6PC3*. *G6PC2* deficient mice show lower fasting blood glucose (Bosma et al., 2020), while
365 humans with mutations in *G6PC3* present with heart defects and neutropenia (Banka et al.,
366 2011; Cheung et al., 2007). An intriguing underlying cellular mechanisms for neutropenia in
367 patients with mutations in *G6PC3* has been proposed (Veiga-da-Cunha et al., 2019), namely
368 the accumulation of 1,5-anhydroglucitol-6-phosphate (1,5AG6P), a toxic metabolite derived
369 from a common circulating food compound (1,5-anhydroglucitol). This is consistent with the
370 observation that *G6PC3*$^{-/-}$ neutrophils express numerous markers indicative of ER stress, while
371 also exhibiting glycosylation defects (Hayee et al., 2011). Thus, it appears that the main role
372 of G6PC3 in neutrophils is to remove a metabolite that is detrimental to optimal physiological
373 processes within these cells. Alternative - and potentially neuronal - roles for G6P enzymes
374 are also indicated by evolutionary arguments, because the *G6P* genes came into existence in
375 Cnidaria, one of the first animal lineages that possessed neuronal cell types, but lacked organs
376 comparable to the liver or even a basic circulatory system (Miyamoto and Amrein, 2017).
377
378 **FMRFamide signaling is essential to build up muscle glycogen stores**
379 Our investigations have identified a primary function for FMRFamides in glycogen
380 metabolism. Under ad libitum feeding conditions, *wild type* flies establish considerable
381 glycogen stores, which can be mobilized in the form of glucose when food is scarce. In
382 contrast, *G6P*^{MIC}, *ΔFMRFa* and *FMRFaR*^{MB04659} mutant flies generate only about half the
383 amount of glycogen in the jump muscle (Figure 7B) and consequently are unable to maintain
384 whole body glucose homeostasis when deprived of food. Thus, FMRFa signaling is essential
385 during normal feeding conditions to assure that glycogen stores are established in the jump
386 muscle.
387 Sugar homeostasis is remarkably well-conserved between mammals and insects.
388 While in mammals, where counteracting hormones - insulin and glucagon – are secreted from
389 pancreatic β and α cells to maintain blood sugar balance, fruit flies use counterbalancing

390 peptides secreted from peptidergic neurons in the CNS for the same process - ILPs and
391 adipokinetic hormone (AKH, the fly ortholog of mammalian glucagon)(reviewed by Kim et al.,
392 2021). An increase in circulating sugars or lipids triggers insulin and ILP secretion from β cells
393 and the IPCs, respectively, which in turn leads to the build-up of fat and glycogen stores in
394 muscle and adipose tissue. When blood and hemolymph sugar levels are low, glucagon and
395 AKH secretion from pancreatic α cells and the Corpora Cardiaca (CC) increases, which
396 ultimately leads to the mobilization of stored fat and glycogen in mammals and insects,
397 respectively. In the fly, the secretion of ILPs and AKH is coordinated by the CN neurons that
398 directly communicate with IPCs and CC neurons, activating the former while suppressing the
399 latter in response to high brain hemolymph glucose levels (Oh et al., 2019). While no direct
400 neural connections between *FMRFa*^{G6P} neurons and IPCs, CC or CN neurons are apparent, it
401 has become evident that multiple, possibly independent, NP signaling pathways control
402 carbohydrate metabolism. Indeed, a third brain sugar sensor was identified in the posterior
403 superior lateral protocerebrum (Miyamoto et al., 2012). This sensor is activated by a spike of
404 the low abundant hemolymph sugar fructose, via the evolutionarily conserved gustatory
405 receptor Gr43a (Fujii et al., 2023). These neurons, which intriguingly express yet another NP
406 (corazonin; Miyamoto and Amrein, 2014), trigger opposite feeding behaviors, promoting food
407 intake when flies are starved, but suppressing food intake when satiated.

408 Our analysis has shown that *FMRFaR* expression is restricted to the jump muscle and
409 the CNS, an observation supported by the "aging fly atlas" (Lu et al., 2023), but this does not
410 exclude the possibility that other tissues might be modulated by FMRFamides. For example,
411 indirect signaling from the jump muscle might lead to larger glycogen stores in other tissues
412 such the indirect flight muscle or the adipose, or FMRFamides might signal to yet unknow
413 peptide receptors. In this context, we note that both *G6P* and *FMRFa* mutant flies, but not
414 *FRMFaR* mutant flies, exhibit impaired climbing ability, suggesting that the *FMRFa*^{G6P} neurons
415 might impact metabolic processes through *FMRFaR* independent signaling pathways
416 (Supplementary Figure 5). Indeed, Song and colleagues showed that a cysteine rich protein
417 diet upregulates FMRFa signaling, which promotes energy expenditure and reduces food
418 intake, resulting in overall loss of fat in the adipose tissue (Song et al., 2023). Their paradigm
419 was based on dietary intervention (high cysteine diet), while our study investigated the
420 function (and loss thereof) of *FMRFa* signaling under normal feeding and starvation
421 conditions. It will be interesting to see whether, and if so, how different metabolic roles of

422 *FMRFa* are interconnected. In another recent report, Ravi and colleagues identified a role for
423 the FMRFaR in the CNS, establishing its requirement in dopaminergic neurons for sustained
424 flight. However, possible metabolic deficits in these flies or the involvement of FMRFamides
425 as signaling molecules was not investigated. Yet, it is likely that energy for sustained flight
426 also requires stored glycogen, provided from the indirect flight muscle or other organs, such
427 as the adipose. Indeed, muscle has gained considerable attention as a metabolic hub
428 communicating with other organs, including the brain, gut and adipose tissue (Demontis et
429 al., 2013, 2013; Gomarasca et al., 2020; Rai and Demontis, 2016; Zhao et al., 2020; Zhao and
430 Karpac, 2017). Thus, our study and those by Ravi and Song and colleagues have implicated
431 *FMRFa* signaling as one likely source in the regulation of different, yet possibly intersecting,
432 nutrient metabolic signaling processes across different organ systems.
433
434 **FIGURE LEGENDS**
435
436 **Figure 1. *G6P* is co-expressed in diverse subsets of peptidergic neurons.**
437 **A-I)** Antibody staining of the brain **(A-F)** and in the thoracic ganglia **(G-I)** of *G6P-GAL4; UAS-*
438 *mCD8GFP* flies using anti-GFP antibody and antibodies against the indicated
439 neuropeptides. *G6P-GAL4* is expressed in about 14 neurons in the brain, including a pair
440 of large, centrally located NPF neurons **(B)** and a pair of large Orcokinin-A expressing
441 neurons **(C)**, two IPNa **(D)** and four PDF neurons **(E)** which correspond l-LNvs. In the
442 thoracic ganglia, *G6P-GAL4* and is expressed in about 10 to 16 neurons, including at least
443 two pairs of FMRFa neurons **(H)** and three pairs of IPNa neurons **(I)**.
444 **J)** Expression summary of *G6P-GAL4* neurons and relevant NP. Co-expressing neurons are
445 outlined with a broken line. Note that all *G6P-GAL4* neurons are of the large variety.
446
447 **Figure 2. G6P mediates whole-body glucose homeostasis through FMRFa neurons.**
448 **A)** Silencing of all *G6P-GAL4* neurons or *GMR18C05-GAL4* (i.e. *FMRFa* expressing neurons;
449 see Figure 3 and Supplementary Figure 1) using *UAS-Kir2.1*, but not silencing of any other
450 subgroup, significantly reduces whole body glucose levels. *GMR13H04-GAL4* is expressed
451 in $OrcoA^{G6P}$ neurons, *GMR37G02-GAL4* in $IPNa^{Br_G6P}$ neurons, *GMR39A01-GAL4* in
452 $IPNa^{Th_G6P}$ neurons and *GMR18C05-GAL4* in $FMRFa^{G6P}$ neurons. Asterisks indicate

453 *P<0.05 using Kruskal-Wallis with Dunn's post-hoc test; n=8-10. Error bars represent
454 standard error.
455 **B)** *G6P* is required in *FMRFa* neurons for whole body glucose homeostasis in starved flies.
456 Under fed conditions, both *wild-type* and *G6P* mutant flies maintain glucose levels (left).
457 However, when starved for 24 hours, *G6P* mutant flies exhibit significantly reduced
458 whole body glucose levels, a phenotype rescued when a *UAS-G6P* transgene is expressed
459 in $FMRFa^{G6P}$ neurons under the control of *GMR18C05-GAL4*. Asterisks indicate *P<0.05
460 using Kruskal-Wallis with Dunn's post-hoc test; n=9-12. Error bars represent standard
461 error.
462 **C)** Structure of the second, ORF containing exon of the wild type *FMRFa* gene and the
463 *FMRFa[P]* and *ΔFMRFa* mutation. Exon 2 contains all 14 FMRFamides and FMRFamide-
464 related peptides. The P-element in *FMRFa[P]* is inserted in the 11th peptide, while all
465 peptides are deleted in *ΔFMRFa*. The first, non-coding exon is not shown.
466 **D)** FMRFamides are required for whole body glucose homeostasis. Like *G6P* mutants,
467 *FMRFa[P]* mutants have significantly lower glucose levels in starved but not fed
468 conditions. *ΔFMRFa* mutant flies show lower glucose levels regardless of feeding
469 conditions. Asterisks indicate *P<0.05, **P<0.01 using one-way ANOVA with Kruskal-
470 Wallis using Dunn's post-hoc test; n=8-12. Error bars represent standard error.
471
472 **Figure 3. $FMRFa^{G6P}$ neurons correspond to 8 Tv neurons in the thoracic ganglion**. The split
473 GAL4 system (*G6P-GAL4DBD* and *FMRFa-p65AD*) was used to identify neurons that express
474 both *G6P* and *FMRFa.* The CNS of *G6P-GAL4DBD/FMRFa-p65AD; 10xUAS-mCD8GFP* flies **(A**
475 **and D)** and *GMR18C05-GAL4; UAS-mCD8GFP* flies **(B and E)** was dissected and stained with
476 anti-GFP and anti-FMRFa antibody.
477 **A-B)** Eight neurons in the thoracic ganglion were labeled by the split GAL4 drivers, all of which
478 also express FMRFa (A' and A"). These neurons are also labeled by *GMR18C05-GAL4* (B,
479 B' and B").
480 **C)** Expression summary of GAL4 drivers in the thoracic ganglion. The eight large FMRFa
481 neurons labeled by either the split GAL4 system or *GMR18C05-GAL4* correspond to the
482 Tv neurons shown to express FMRFa (Schneider et al., 1993b).
483 **D- E)** Neither split GAL4 nor *GMR18C05-GAL4* are expressed in any FMRFa neurons in the
484 brain.

485

486 **Figure 4. *G6P* is required to maintain glucose levels in FMRFa neurons of food-deprived flies**.
487 Glucose levels were measured using Glu700KDEL, a FRET-based, ER tagged glucose sensor, in
488 FMRFa neurons in the thoracic ganglion of *GMR18C05-GAL4/UAS-Glu700KDEL* flies. Glucose
489 levels are reduced in starved *G6P* mutant flies, which was rescued in the presence of a *UAS-*
490 *G6P* transgene. Asterisk indicates **P<0.01 using one-way ANOVA with Tukey post hoc test.
491 N=8-17. Error bars represent standard error.

492

493 **Figure 5. G6P positively affects the size of Golgi apparatus in the peptidergic neurons.**
494 The Golgi apparatus was visualized by expressing the GFP tagged Golgi marker UAS-ManII-
495 eGFP. FMRFa staining was used as a proxy for cell body. Golgi size is given as percentage of
496 cell body size (see also Supplementary Figure 4). *FMRFa*^{G6P} neurons were identified using
497 *GMR18C05-GAL4* driving *UAS-ManII-eGFP* expression **(A)** and *NPF*^{G6P} neurons were identified
498 using *NPF-GAL4* driving *UAS-ManII-eGFP* expression **(B)**. Neurons of *G6P*$^{-/-}$ flies have a
499 significantly smaller Golgi apparatus, in fed and starved conditions. This phenotype is rescued
500 *UAS-G6P* transgene expression. Asterisks indicate *P<0.05 using Kruskal-Wallis with Dunn's
501 post-hoc test. N=44-65 for *FMRFa*^{G6P} neurons, N=12-23 for *NPF*^{G6P} neurons. Error bars
502 represent standard error. Scale bars are 4µm.

503

504 **Figure 6: FMRFa neurons require G6P for efficient neuropeptide secretion.**
505 **A-B)** Secreted **(A)** and total amount **(B)** of Anf-GFP was quantified by ELISA (Rat ANP ELISA Kit;
506 abcam, ab108797) in flies expressing *UAS-Anf-GFP* in *FMRFa* neurons (*GMR18C05-GAL4*).
507 Compared to *wild-type* (left bar in each set), the hemolymph of *G6P* mutant flies (center
508 bar) contains significantly lower amounts of Anf-GFP in both the fed and starved flies **(A)**.
509 Secretion of Anf-GFP is rescued in the presence of a *UAS-G6P* transgene (right bar in each
510 set. Total amount of Anf-GFP was unaffected by the presence or absence of G6P **(B)**.
511 **C - D)** Secreted **(C)** and total amount **(D)** of Ilp2HF was quantified in *Ilp2*^{1} *gd2HF* flies, which
512 carry a genetically tagged Ilp2 allele. Ectopic expression of *UAS-G6P* under the control of
513 *dilp2-GAL4* increased Ilp2HF levels in the hemolymph of starved flies **(C)** with concomitant
514 reduction in total Ilp2HF **(D)**. In fed flies, a small increase of total Ilp2HF was observed.
515 Asterisks indicate **P<0.01 using Kruskal-Wallis with Dunn's post-hoc test. N=12 for
516 *FMRFa*^{G6P} neurons. N=9 for IPC. Bars represent standard error.

517

518 **Figure 7: FMRFa acts on the FMRFa receptor to establish glycogen stores in the jump muscle**

519 **A)** *FMRFaR* was visualized using a *GAL4* gene knock in allele (*FMRFaR*$^{2A\text{-}GAL4}$) combined with
520 *UAS-20xUAS-6xGFP*, following anti-GFP staining. Flies show robust expression in the jump
521 muscle and CNS. Preparation was counterstained with Phalloidin (Invitrogen A34055).

522 **B)** Glycogen stores in the jump muscle were significantly smaller in the *FMRFaR*^{MB} mutant
523 flies under starved conditions, while glucose levels remained unchanged.

524 **C)** Glycogen stores were restored to *wild type* levels when *UAS-FMRFaR* was expressed in
525 the jump muscle in *FMRFaR*^{MB} mutant flies also containing *ELAV-GAL80* suppressor.
526 Expression of *UAS-FMRFaR* in the fat body using the *CG-GAL4* driver, however, did not
527 restore glycogen levels in the jump muscle.

528 **D)** Glycogen loss in the jump muscle is also observed in the *G6P*^{MIC} and *ΔFMRFa* mutant
529 flies.

530 Asterisks indicate *P<0.05, **P<0.01 by one-way Kruskal-Wallis with Dunn's post-hoc test.
531 n=7-14. Error bars represent standard error.

532

533 **ACKNOWLEGEMENTS**

534 We thank Dr. Paul Hardin for the *Pdf-GAL4* strain, Dr. Gaiti Hasan for the *UAS-FMRFaR* strain,
535 Dr. Richard Cripps for the *Act79B-GAL4* strain and Dr. Seung Kim for *Ilp2*^{1} *gd2HF* strain. We
536 also thank Dr. Wolf Frommer for the Glu700KDEL plasmid (Addgene plasmid #17867) and Dr.
537 Simon Bullock for pCFD3 plasmid (Addgene plasmid #49410), Dr. Gerald Rubin for the
538 GAL4DBD and p65AD plasmids (Addgene #26233 and #26234). Antibody gifts were provided
539 by Dr. Mizoguchi (anti-Orcokinin), Dr. Thor (anti-IPNa, anti-proFMRFa) and Dr. Hardin (anti-
540 PDF). We thank Anastasia Lucas and Edward Wang for assistance with glycogen
541 measurements and Drs. Dick Nässel and Raquel Sitcheran for valuable comments on the
542 manuscript. We are grateful to Anastasia Lucas and Edward Wang for assistance on the
543 metabolic assays. This work was supported by an NIH grant 1R21NS118118-01 awarded to
544 H.A.

545

546 **MATERIAL AND METHODS**

547

548 **Fly strains and maintenance**

549 Experiments were performed using adult *Drosophila melanogaster* males, aged between 7-
550 14 days. Flies were reared on the standard fly food containing cornmeal, yeast and sugar at
551 23-24˚C. *G6P*^{MI12250} is referred as *G6P*^{MIC}, *FMRFa*^{KG01300} is referred as *FMRFa*^{P}, *FMRFaR*^{MB04659}
552 is referred as *FMRFaR*^{MB}. See supplementary data for detailed genotypes.
553
554 **Quantification and Statistical Analysis**
555 Statistical significance was calculated using Student's t-test or two-tailed Mann-Whitney U
556 test for pairwise comparisons, and one-way ANOVA with Tukey post hoc test or Kruskal-
557 Wallis test with Dunn's post-hoc test for multiple comparisons. Error bars are standard error
558 of the mean (SEM) except where noted. Significance: *p<0.05, **p<0.01, NS: not significant.
559 All replicates are from different biological samples (testing different flies or cells). Image
560 analysis was performed with NIS-Elements software suite. Statistical analysis was performed
561 in Real Statistics Add-Ins in MS Excel and GraphPad PRISM. Number of replicates was 8-10
562 (Figure 2A), 9-12 (Figure 2B), 8-12 (Figure 2D), 12-17 (Figure 4), 51-65 (Figure 5A), 12-23
563 (Figure 5B), 11 (Figure 6A), 9 (Figure 6B), 7-14 (Figure 7B), 12-14 (Figure 7C), 7 (Figure 7D).
564
565 **Molecular Biology**
566 The *UAS-FLII*^{12}*Pglu-700μδ6KDEL* was generated from the expression plasmid pEF/myc/ER
567 *FLII*^{12}*Pglu-700μδ6* (Addgene). The glucose sensor coding sequence was excised using PstI and
568 XbaI. This fragment, along with a fragment encoding an ER targeting module (5'-
569 GAACAGAATTCAGATCTGCCACC**ATG**GGATGGAGCTGTATCATCCTCTTCTTGGTAGCAACAGCTAC
570 AGGCGCGCACTCCCAGGTCCAACTGCAGTCA-3') cut with EcoRI and PstI, were cloned in a three
571 way cloning step into the *pUAST* vector, cut with EcoRI and XbaI. This construct was injected
572 into *w*^{1118} embryos (Bestgene, Inc). For construction of *G6P-GAL4DBD*, the promoter region
573 of *G6P* was amplified from genomic DNA of the *w*^{1118} strain, using 5'-
574 GGCGGCCGCCACTTCGAGAACTTTGGATAGGT-3' and 5'-
575 GGGTACCATCGACTCCAATGTTTTCAGTCTT-3' primers. DNA fragment was cloned into
576 *pBPZpGAL4DBDUw* vector (addgene #26233)(Pfeiffer et al., 2010).
577 For construction of the *FMRFa-p65AD*, the promoter region of *FMRFa* was amplified using 5'-
578 CGTTAACGTTCGAGGTCGACTCTGCAGACGTGGTTTTCG-3' and 5'-
579 CGTTAACGTTCGAGGTCGACTCTGCAGACGTGGTTTTCG-3' primers (Schneider et al., 1993a).

580 DNA fragment was cloned into pBPp65ADZpUw (addgene #26234) (Pfeiffer Rubin 2010). All
581 constructs were injected into w^{1118} embryos (Bestgene, Inc).
582 Generation of *FMRFa* null mutations: *FMRFa* mutation was generated using CRISPR/Cas9
583 mutagenesis. The guide RNA (gRNA) was designed to anneal to nucleotides 175 to 194
584 downstream of the translation start codon (nucleotide 1) of the *FMRFa* gene.
585 Complementary oligos were annealed and cloned into the pCFD3-dU6:3gRNA vector
586 (Addgene #49410). The vector was introduced into *vermillion* (*v*) strain and crossed with
587 *Act5C-Cas9* flies (Bloomington #54590). Approximately 10 progenies were collected and
588 established as independent lines. Each fly within the established lines were sequenced. The
589 deletion in *ΔFMRFa* removes almost 900 nucleotides (175 to 1063) encoding all 14 *FMRFa*
590 peptides. Glu700KDEL was a gift from Dr. Wolf Frommer (Addgene plasmid #17867).
591
592 **Immunostaining**
593 Fly brains and thoracic ganglions were dissected in 1xPBS and then fixed in 4%
594 paraformaldehyde with 0.2% Triton X-100 for 30 min at room temperature. Fixed brains were
595 washed three times with PBS containing 0.2% Triton X-100. The samples were incubated in
596 blocking buffer (5% heat-inactivated goat serum) with 0.2% Triton X-100 for 30 min at room
597 temperature. Then, samples were incubated with 1/1000 diluted primary antibodies for 1-2
598 days at 4 ˚C. Samples were washed three times with PBS with 0.2% Triton X-100 and
599 incubated with 1/1000 diluted secondary antibodies for 1-2 days at 4 ˚C. Samples were
600 washed three times with PBS with 0.2% Triton X-100 and mounting solution (Vectashield)
601 was added. Primary antibodies used in this study include chicken anti-GFP (Thermo Fisher
602 Scientific), rabbit anti-mCherry (BioVision), rabbit anti-NPF (RayBiotech), mouse anti-
603 Orcokinin-A (gift from Dr. Mizoguchi), rabbit anti-IPNa (gift from Dr. Thor), rabbit anti-Pdf
604 (gift from Dr. Hardin), rabbit anti-FMRFa (RayBiotech). Secondary antibodies were anti-
605 chicken Alexa488 (Thermo Fisher Scientific), anti-rabbit Alexa555 (Thermo Fisher Scientific)
606 and anti-mouse Cy3 (The Jackson laboratory).
607
608 ***In vivo* Glucose imaging**
609 Glucose imaging of FMRF neuron in the thoracic ganglion was conducted analogously as
610 reported for NPF brain neurons, with the following modifications: the thoracic ganglion was
611 extracted from the thorax while liquid silicone was applied over the entire preparation to

612 prevent desiccation and preserve intracellular homeostatic conditions. Imaging was
613 performed with a Nikon Eclipse Ti inverted microscope using 20x water objective, a dichroic
614 filter (Nikon; 89002), excitation and emission filter wheels with four Chroma filters ET430/24x
615 (#234435), ET500/20x (#235394), ET470/24m (#234331) and ET535/30m (Chroma #239226).
616 The light source was a Lumen 200 lamp (Prior Scientific Inc). Data acquisition was performed
617 with NIS-Elements software (Nikon). For each data point, three images were sequentially
618 obtained to calculate FRET (420-445 nm for CFP excitation and 458-482 nm for CFP emission
619 with 400 ms exposure (Dd), 420-445 nm for CFP excitation and 520-550 nm for YFP emission
620 with 100 ms exposure (Da), 491-508 nm for YFP excitation and 520-550 nm for YFP emission
621 with 100 ms exposure (Aa)). Dd and Aa were used to calculate false FRET signals generated
622 by CFP and YFP molecules alone, respectively. Spillover factors for CFP (0.290) and YFP (0.095)
623 were experimentally established (Miyamoto and Amrein, 2019). For data analysis, adjacent
624 area of cell bodies was subtracted as a background. FRET efficiency was calculated using a
625 following formula; (Da-0.29xDd-0.095xAa)/Dd.
626
627 **Golgi size measurement**
628 The Golgi apparatus was visualized using *UAS-ManII-eGFP* expressed under the control of
629 respective GAL4 drivers. Golgi and NP staining was performed as described in
630 Immunostaining except for using 4% paraformaldehyde with 0.01% Triton X-100 for fixation.
631 All images were taken using a Nikon A1 confocal microscope with 60 x oil lens. Golgi and NP
632 images were stacked (0.5 μm section intervals) and analyzed using ImageJ. Background was
633 subtracted by thresholding using MaxEntropy for Golgi, Huang or Mean for NPs, and
634 remained pixel numbers were counted. Golgi area was determined as the fraction of the area
635 positive for NP, which served as a proxy for the cytosol.
636
637 **Metabolic Analyses**
638 Glucose/trehalose measurements: For glucose and trehalose measurements, a single male
639 fly was homogenized in 100 μl of water. After heat-inactivation at 95 ˚C for 5 min, non-soluble
640 debris was removed by centrifugation for 10 minutes at 14000 rpm and soluble fraction was
641 transferred to a new Eppendorf tube. 5 μl of the soluble fraction was used for determination
642 of glucose and trehalose content, respectively. Glucose was determined by adding 100 μl of

643 Infinity™ Glucose Hexokinase Reagent (Thermo Scientific) to 5 μl of the soluble fraction for
644 10 minutes at 37 ˚C. Absorbance was measured at 340 nm using a Genesys 20
645 spectrophotometer (Thermo Scientific) and quantified against a standard glucose curve. For
646 trehalose measurement, 5 μl of porcine kidney trehalase (2.3 units/mg; T8778-1UN, Sigma)
647 was added to 5 μl of the soluble fraction for 30 minutes at 37 ˚C, followed the addition of 100
648 μl of the Infinity™ Glucose Hexokinase Reagent. Absorbance was measured as for glucose,
649 and final trehalose amount was determined by deducting glucose content of the same fly
650 sample. Fed flies were taken straight from standard food, while starved flies are flies kept on
651 1% agarose for 24 hours prior measurement.
652 Glycogen measurement: Adult males were anesthetized using CO_2. The abdomen and head
653 were removed, the thorax separated into the dorsal (flight muscle) and the ventral halves
654 (jump muscle). Jump muscles from three flies were placed into an Eppendorf tube containing
655 50 µl of 0.2 % NP-40 and stored at - 80 ˚C, until further processing. For measurements,
656 samples were thawed, homogenized using a plastic pestle, and non-soluble debris was
657 separated by centrifugation at 4 ˚C for 20 minutes at 14000 rpm. 5 µl of the supernatant was
658 incubated with 5 µg of amyloglucosidase (Sigma- Aldrich A1602) with 50 mM Na acetate for
659 30 minutes at 37 ˚C. The aliquot was mixed with 100 µl of Infinity™ Glucose Hexokinase
660 Reagent and incubated for 10 minutes at 37 ˚C, before absorbance was measured at 340 nm.
661 Glycogen amount was obtained by subtraction of free glucose which was determined by
662 measuring 340 nm absorbance of 5 µl of the same sample in the absence of amyloglucosidase.
663 Samples were normalized to total amount of protein, which was determined using 20 µl of
664 supernatant, to which with 20 µl water was added. 2.5 µl of this was mixed with 100 µl of
665 Bradford reagent (Bio-Rad #5000205) and absorbance was taken at 595 nm to calculate
666 protein concentration against a standard curve.
667
668 **Hemolymph neuropeptide measurements**
669 Hemolymph extraction was performed as described by Davoodi and colleagues (Davoodi et
670 al., 2019). Briefly, abdomens of ten flies were punctured at the posterior end and transferred
671 in an iced Eppendorf tube containing 60 µl of PBS with 0.2 % Tween20. Flies were submerged
672 in the buffer by spinning samples for 1 minute at 3000 × g in a microcentrifuge, followed by
673 vortexing at speed 10 (Fisher Scientific Vortex mixer) for 10 minutes. Debris was removed by

674 centrifugation for 1 minute at 3000 × g, and the supernatant (hemolymph) was transferred
675 to a new tube.
676 ELISA was performed in triplicates using the ANP ELISA kit (Abcam #ab108797). Briefly, 50 µl
677 of samples and standard titration in the range from 0.008 ng/mL to 2 ng/mL were added to
678 each precoated well. The plate was fully sealed and incubated for 2-3 hours, followed by 4-5
679 washes with 200 µl of wash buffer. 50 µl of Biotinylated ANP antibody was added and
680 incubated for 2 hours at room temperature. The wells were washed three times and 50 µl of
681 Streptavidin-Peroxidase conjugate was added. After 30 minutes, the wells were washed once.
682 50 µl of chromogen substrate was added and incubated for 20 minutes or until the desired
683 blue color was achieved, after which the reaction was terminated by adding 50 µl of the stop
684 solution. Absorbance was measured immediately at 450nm using a microplate reader (BioTek
685 Instruments Inc).
686 Measurement of Ilp2HF in the hemolymph was performed using the *Ilp2*^{1} *gd2HF* flies as
687 described previously (Park et al 2014). Plates (Nunc Immuno clear modules; Thermo Fisher
688 Scientific 468667) were coated with anti-Flag antibody (Sigma-Aldrich F1804) diluted in 0.2 M
689 sodium carbonate/bicarbonate buffer (pH 9.4) to a final concentration of 2.5µg/mL. Plates
690 were incubated overnight at 4 ˚C, washed twice using PBS containing 0.2% Tween 20. The
691 wells were coated with 350µL PBS containing 2% BSA overnight, washed three times with PBS
692 containing 0.2% Tween 20. The hemolymph was extracted in the same way as Anf-GFP,
693 described above. 50µL of hemolymph containing solution or FLAG(GS)HA peptide standard
694 (DYKDDDDKGGGGSYPYDVPDYAamide, life-Tein LLC) was mixed with 50µl of PBS containing
695 1% Tween20 and 5ng/mL anti-HA-Peroxidase 3F10 antibody (Roche #12013819001) and
696 transferred to the wells. Plates were sealed and incubated overnight at 4 ˚C. Samples were
697 removed and wells were washed six times with PBS with 0.2% Tween20. 100µL of 1-Step Ultra
698 TMB ELISA substrate (Thermo Fisher Scientific #34028) was added to each well, and plates
699 were gently agitated for 30 minutes at room temperature. The reaction was stopped by
700 adding 100µL of 2M sulfuric acid, and absorbance was measured immediately at 450nm.
701
702 **Climbing assay**
703 The climbing assay was performed as reported by Ali and colleagues (Ali et al., 2011).
704 Approximately 15-20 male flies were placed in a culture plastic vial containing regular food
705 (fed conditions) or plain agarose (starved conditions) 24 hours prior to testing. Flies were

transferred into an empty vial with a line marker 8 cm from the bottom, and tested by tapping them down gently to the bottom. The number of flies climbing up to marked within 10 seconds were counted.

709 **REFERENCES**

710 Ali, Y.O., Escala, W., Ruan, K., Zhai, R.G., 2011. Measurement of the Relations between
711 Chromosomes and Behavior. Journal of visualized experiments: JoVE.
712 https://doi.org/10.3791/2504
713 Baines, R.A., Uhler, J.P., Thompson, A., Sweeney, S.T., Bate, M., 2001. Altered electrical
714 properties in Drosophila neurons developing without synaptic transmission. J
715 Neurosci 21, 1523–1531. https://doi.org/10.1523/JNEUROSCI.21-05-01523.2001
716 Banka, S., Chervinsky, E., Newman, W.G., Crow, Y.J., Yeganeh, S., Yacobovich, J., Donnai, D.,
717 Shalev, S., 2011. Further delineation of the phenotype of severe congenital
718 neutropenia type 4 due to mutations in G6PC3. Eur J Hum Genet 19, 18–22.
719 https://doi.org/10.1038/ejhg.2010.136
720 Bosma, K.J., Rahim, M., Singh, K., Goleva, S.B., Wall, M.L., Xia, J., Syring, K.E., Oeser, J.K.,
721 Poffenberger, G., McGuinness, O.P., Means, A.L., Powers, A.C., Li, W.-H., Davis, L.K.,
722 Young, J.D., O'Brien, R.M., 2020. Pancreatic islet beta cell-specific deletion of G6pc2
723 reduces fasting blood glucose. J Mol Endocrinol 64, 235–248.
724 https://doi.org/10.1530/JME-20-0031
725 Brussaard, A.B., Kits, K.S., Ter Maat, A., Van Minnen, J., Moed, P.J., 1988. Dual inhibitory
726 action of FMRFamide on neurosecretory cells controlling egg laying behavior in the
727 pond snail. Brain Res 447, 35–51. https://doi.org/10.1016/0006-8993(88)90963-8
728 Bryantsev, A.L., Baker, P.W., Lovato, T.L., Jaramillo, M.S., Cripps, R.M., 2012. Differential
729 requirements for Myocyte Enhancer Factor-2 during adult myogenesis in Drosophila.
730 Dev Biol 361, 191–207. https://doi.org/10.1016/j.ydbio.2011.09.031
731 Cheung, Y.Y., Kim, S.Y., Yiu, W.H., Pan, C.-J., Jun, H.-S., Ruef, R.A., Lee, E.J., Westphal, H.,
732 Mansfield, B.C., Chou, J.Y., 2007. Impaired neutrophil activity and increased
733 susceptibility to bacterial infection in mice lacking glucose-6-phosphatase-beta. J Clin
734 Invest 117, 784–793. https://doi.org/10.1172/JCI30443
735 Chung, B.Y., Ro, J., Hutter, S.A., Miller, K.M., Guduguntla, L.S., Kondo, S., Pletcher, S.D.,
736 2017. Drosophila Neuropeptide F Signaling Independently Regulates Feeding and
737 Sleep-Wake Behavior. Cell Rep 19, 2441–2450.
738 https://doi.org/10.1016/j.celrep.2017.05.085
739 Davoodi, S., Galenza, A., Panteluk, A., Deshpande, R., Ferguson, M., Grewal, S., Foley, E.,
740 2019. The Immune Deficiency Pathway Regulates Metabolic Homeostasis in
741 Drosophila. J Immunol 202, 2747–2759. https://doi.org/10.4049/jimmunol.1801632
742 Demontis, F., Piccirillo, R., Goldberg, A.L., Perrimon, N., 2013. The influence of skeletal
743 muscle on systemic aging and lifespan. Aging Cell 12, 943–949.
744 https://doi.org/10.1111/acel.12126
745 Deng, B., Li, Q., Liu, X., Cao, Y., Li, B., Qian, Y., Xu, R., Mao, R., Zhou, E., Zhang, W., Huang, J.,
746 Rao, Y., 2019. Chemoconnectomics: Mapping Chemical Transmission in Drosophila.
747 Neuron 101, 876-893.e4. https://doi.org/10.1016/j.neuron.2019.01.045
748 Fisher, T., Lin, C.H., Kaczmarek, L.K., 1993. The peptide FMRFa terminates a discharge in
749 Aplysia bag cell neurons by modulating calcium, potassium, and chloride
750 conductances. J Neurophysiol 69, 2164–2173.
751 https://doi.org/10.1152/jn.1993.69.6.2164
752 Fujii, S., Ahn, J.-E., Jagge, C., Shetty, V., Janes, C., Mohanty, A., Slotman, M., Adelman, Z.N.,
753 Amrein, H., 2023. RNA Taste is Conserved in Dipteran Insects. J Nutr S0022-
754 3166(23)35477–4. https://doi.org/10.1016/j.tjnut.2023.03.010

755 Gauthier, S.A., Hewes, R.S., 2006. Transcriptional regulation of neuropeptide and peptide
756 hormone expression by the Drosophila dimmed and cryptocephal genes. J Exp Biol
757 209, 1803–1815. https://doi.org/10.1242/jeb.02202
758 Gomarasca, M., Banfi, G., Lombardi, G., 2020. Myokines: The endocrine coupling of skeletal
759 muscle and bone. Adv Clin Chem 94, 155–218.
760 https://doi.org/10.1016/bs.acc.2019.07.010
761 Hardt, B., Völker, C., Mundt, S., Salska-Navarro, M., Hauptmann, M., Bause, E., 2005. Human
762 endo-alpha1,2-mannosidase is a Golgi-resident type II membrane protein. Biochimie
763 87, 169–179. https://doi.org/10.1016/j.biochi.2004.11.004
764 Hayee, B., Antonopoulos, A., Murphy, E.J., Rahman, F.Z., Sewell, G., Smith, B.N., McCartney,
765 S., Furman, M., Hall, G., Bloom, S.L., Haslam, S.M., Morris, H.R., Boztug, K., Klein, C.,
766 Winchester, B., Pick, E., Linch, D.C., Gale, R.E., Smith, A.M., Dell, A., Segal, A.W.,
767 2011. G6PC3 mutations are associated with a major defect of glycosylation: a novel
768 mechanism for neutrophil dysfunction. Glycobiology 21, 914–924.
769 https://doi.org/10.1093/glycob/cwr023
770 Herzog, H., Darby, K., Ball, H., Hort, Y., Beck-Sickinger, A., Shine, J., 1997. Overlapping gene
771 structure of the human neuropeptide Y receptor subtypes Y1 and Y5 suggests
772 coordinate transcriptional regulation. Genomics 41, 315–319.
773 https://doi.org/10.1006/geno.1997.4684
774 Hewes, R.S., Park, D., Gauthier, S.A., Schaefer, A.M., Taghert, P.H., 2003. The bHLH protein
775 Dimmed controls neuroendocrine cell differentiation in Drosophila. Development
776 130, 1771–1781. https://doi.org/10.1242/dev.00404
777 Higuchi, H., Hasegawa, A., Yamaguchi, T., 2005. Transcriptional regulation of neuronal genes
778 and its effect on neural functions: transcriptional regulation of neuropeptide Y gene
779 by leptin and its effect on feeding. J Pharmacol Sci 98, 225–231.
780 https://doi.org/10.1254/jphs.fmj05001x6
781 Hook, V., Funkelstein, L., Lu, D., Bark, S., Wegrzyn, J., Hwang, S.-R., 2008. Proteases for
782 processing proneuropeptides into peptide neurotransmitters and hormones. Annu
783 Rev Pharmacol Toxicol 48, 393–423.
784 https://doi.org/10.1146/annurev.pharmtox.48.113006.094812
785 Husain, Q.M., Ewer, J., 2004. Use of targetable gfp-tagged neuropeptide for visualizing
786 neuropeptide release following execution of a behavior. J Neurobiol 59, 181–191.
787 https://doi.org/10.1002/neu.10309
788 Kim, S.K., Tsao, D.D., Suh, G.S.B., Miguel-Aliaga, I., 2021. Discovering signaling mechanisms
789 governing metabolism and metabolic diseases with Drosophila. Cell Metab 33, 1279–
790 1292. https://doi.org/10.1016/j.cmet.2021.05.018
791 Kneen, M., Farinas, J., Li, Y., Verkman, A.S., 1998. Green fluorescent protein as a noninvasive
792 intracellular pH indicator. Biophys J 74, 1591–1599. https://doi.org/10.1016/S0006-
793 3495(98)77870-1
794 Kondylis, V., Rabouille, C., 2009. The Golgi apparatus: lessons from Drosophila. FEBS Lett
795 583, 3827–3838. https://doi.org/10.1016/j.febslet.2009.09.048
796 Kovac, S., Shulkes, A., Baldwin, G.S., 2009. Peptide processing and biology in human disease.
797 Curr Opin Endocrinol Diabetes Obes 16, 79–85.
798 https://doi.org/10.1097/MED.0b013e3283202555
799 Landayan, D., Wang, B.P., Zhou, J., Wolf, F.W., 2021. Thirst interneurons that promote water
800 seeking and limit feeding behavior in Drosophila. Elife 10.
801 https://doi.org/10.7554/eLife.66286

802 Lear, B.C., Zhang, L., Allada, R., 2009. The neuropeptide PDF acts directly on evening
803 pacemaker neurons to regulate multiple features of circadian behavior. PLoS Biol 7,
804 e1000154. https://doi.org/10.1371/journal.pbio.1000154
805 Lee, K.-S., You, K.-H., Choo, J.-K., Han, Y.-M., Yu, K., 2004. Drosophila short neuropeptide F
806 regulates food intake and body size. J Biol Chem 279, 50781–50789.
807 https://doi.org/10.1074/jbc.M407842200
808 Lenz, O., Xiong, J., Nelson, M.D., Raizen, D.M., Williams, J.A., 2015. FMRFamide signaling
809 promotes stress-induced sleep in Drosophila. Brain Behav Immun 47, 141–148.
810 https://doi.org/10.1016/j.bbi.2014.12.028
811 Liu, W., Ganguly, A., Huang, J., Wang, Y., Ni, J.D., Gurav, A.S., Aguilar, M.A., Montell, C.,
812 2019. Neuropeptide F regulates courtship in Drosophila through a male-specific
813 neuronal circuit. Elife 8. https://doi.org/10.7554/eLife.49574
814 Lu, T.-C., Brbić, M., Park, Y.-J., Jackson, T., Chen, J., Kolluru, S.S., Qi, Y., Katheder, N.S., Cai,
815 X.T., Lee, S., Chen, Y.-C., Auld, N., Liang, C.-Y., Ding, S.H., Welsch, D., D'Souza, S.,
816 Pisco, A.O., Jones, R.C., Leskovec, J., Lai, E.C., Bellen, H.J., Luo, L., Jasper, H., Quake,
817 S.R., Li, H., 2023. Aging Fly Cell Atlas identifies exhaustive aging features at cellular
818 resolution. Science 380, eadg0934. https://doi.org/10.1126/science.adg0934
819 Luan, H., Peabody, N.C., Vinson, C.R., White, B.H., 2006. Refined spatial manipulation of
820 neuronal function by combinatorial restriction of transgene expression. Neuron 52,
821 425–436. https://doi.org/10.1016/j.neuron.2006.08.028
822 Lundquist, T., Nässel, D.R., 1990. Substance P-, FMRFamide-, and gastrin/cholecystokinin-
823 like immunoreactive neurons in the thoraco-abdominal ganglia of the flies
824 Drosophila and Calliphora. J Comp Neurol 294, 161–178.
825 https://doi.org/10.1002/cne.902940202
826 Matsuda, H., Yamada, T., Yoshida, M., Nishimura, T., 2015. Flies without trehalose. J Biol
827 Chem 290, 1244–1255. https://doi.org/10.1074/jbc.M114.619411
828 Miyamoto, T., Amrein, H., 2019. Neuronal Gluconeogenesis Regulates Systemic Glucose
829 Homeostasis in Drosophila melanogaster. Curr Biol 29, 1263-1272.e5.
830 https://doi.org/10.1016/j.cub.2019.02.053
831 Miyamoto, T., Amrein, H., 2017. Gluconeogenesis: An ancient biochemical pathway with a
832 new twist. Fly (Austin) 11, 218–223.
833 https://doi.org/10.1080/19336934.2017.1283081
834 Miyamoto, T., Amrein, H., 2014. Diverse roles for the Drosophila fructose sensor Gr43a. Fly
835 (Austin) 8, 19–25. https://doi.org/10.4161/fly.27241
836 Miyamoto, T., Slone, J., Song, X., Amrein, H., 2012. A fructose receptor functions as a
837 nutrient sensor in the Drosophila brain. Cell 151, 1113–1125.
838 https://doi.org/10.1016/j.cell.2012.10.024
839 Nässel, D.R., Zandawala, M., 2019. Recent advances in neuropeptide signaling in Drosophila,
840 from genes to physiology and behavior. Prog Neurobiol 179, 101607.
841 https://doi.org/10.1016/j.pneurobio.2019.02.003
842 Oh, Y., Lai, J.S.-Y., Mills, H.J., Erdjument-Bromage, H., Giammarinaro, B., Saadipour, K.,
843 Wang, J.G., Abu, F., Neubert, T.A., Suh, G.S.B., 2019. A glucose-sensing neuron pair
844 regulates insulin and glucagon in Drosophila. Nature 574, 559–564.
845 https://doi.org/10.1038/s41586-019-1675-4
846 Paradis, S., Sweeney, S.T., Davis, G.W., 2001. Homeostatic control of presynaptic release is
847 triggered by postsynaptic membrane depolarization. Neuron 30, 737–749.
848 https://doi.org/10.1016/s0896-6273(01)00326-9

849 Parisky, K.M., Agosto, J., Pulver, S.R., Shang, Y., Kuklin, E., Hodge, J.J.L., Kang, K., Liu, X.,
850 Garrity, P.A., Rosbash, M., Griffith, L.C., 2008. PDF cells are a GABA-responsive wake-
851 promoting component of the Drosophila sleep circuit. Neuron 60, 672–682.
852 https://doi.org/10.1016/j.neuron.2008.10.042
853 Park, S., Alfa, R.W., Topper, S.M., Kim, G.E.S., Kockel, L., Kim, S.K., 2014. A genetic strategy
854 to measure circulating Drosophila insulin reveals genes regulating insulin production
855 and secretion. PLoS Genet 10, e1004555.
856 https://doi.org/10.1371/journal.pgen.1004555
857 Pauls, D., Chen, J., Reiher, W., Vanselow, J.T., Schlosser, A., Kahnt, J., Wegener, C., 2014.
858 Peptidomics and processing of regulatory peptides in the fruit fly Drosophila. EuPA
859 Open Proteomics 3, 114–127.
860 Pfeiffer, B.D., Ngo, T.-T.B., Hibbard, K.L., Murphy, C., Jenett, A., Truman, J.W., Rubin, G.M.,
861 2010. Refinement of tools for targeted gene expression in Drosophila. Genetics 186,
862 735–755. https://doi.org/10.1534/genetics.110.119917
863 Predel, R., Wegener, C., Russell, W.K., Tichy, S.E., Russell, D.H., Nachman, R.J., 2004.
864 Peptidomics of CNS-associated neurohemal systems of adult Drosophila
865 melanogaster: a mass spectrometric survey of peptides from individual flies. J Comp
866 Neurol 474, 379–392. https://doi.org/10.1002/cne.20145
867 Rai, M., Demontis, F., 2016. Systemic Nutrient and Stress Signaling via Myokines and
868 Myometabolites. Annu Rev Physiol 78, 85–107. https://doi.org/10.1146/annurev-
869 physiol-021115-105305
870 Ravi, P., Trivedi, D., Hasan, G., 2018. FMRFa receptor stimulated Ca2+ signals alter the
871 activity of flight modulating central dopaminergic neurons in Drosophila
872 melanogaster. PLoS Genet 14, e1007459.
873 https://doi.org/10.1371/journal.pgen.1007459
874 Renn, S.C., Park, J.H., Rosbash, M., Hall, J.C., Taghert, P.H., 1999. A pdf neuropeptide gene
875 mutation and ablation of PDF neurons each cause severe abnormalities of behavioral
876 circadian rhythms in Drosophila. Cell 99, 791–802. https://doi.org/10.1016/s0092-
877 8674(00)81676-1
878 Rholam, M., Fahy, C., 2009. Processing of peptide and hormone precursors at the dibasic
879 cleavage sites. Cell Mol Life Sci 66, 2075–2091. https://doi.org/10.1007/s00018-009-
880 0007-5
881 Schneider, L.E., Roberts, M.S., Taghert, P.H., 1993a. Cell type-specific transcriptional
882 regulation of the Drosophila FMRFamide neuropeptide gene. Neuron 10, 279–291.
883 https://doi.org/10.1016/0896-6273(93)90318-l
884 Schneider, L.E., Sun, E.T., Garland, D.J., Taghert, P.H., 1993b. An immunocytochemical study
885 of the FMRFamide neuropeptide gene products in Drosophila. J Comp Neurol 337,
886 446–460. https://doi.org/10.1002/cne.903370308
887 Shao, L., Saver, M., Chung, P., Ren, Q., Lee, T., Kent, C.F., Heberlein, U., 2017. Dissection of
888 the Drosophila neuropeptide F circuit using a high-throughput two-choice assay.
889 Proc Natl Acad Sci U S A 114, E8091–E8099.
890 https://doi.org/10.1073/pnas.1710552114
891 Silva, V., Palacios-Muñoz, A., Volonté, M., Frenkel, L., Ewer, J., Ons, S., 2021. Orcokinin
892 neuropeptides regulate reproduction in the fruit fly, Drosophila melanogaster. Insect
893 Biochem Mol Biol 139, 103676. https://doi.org/10.1016/j.ibmb.2021.103676

894 Song, T., Qin, W., Lai, Z., Li, H., Li, D., Wang, B., Deng, W., Wang, T., Wang, L., Huang, R.,
895 2023. Dietary cysteine drives body fat loss via FMRFamide signaling in Drosophila
896 and mouse. Cell Res 33, 434–447. https://doi.org/10.1038/s41422-023-00800-8
897 Taghert, P.H., Hewes, R.S., Park, J.H., O'Brien, M.A., Han, M., Peck, M.E., 2001. Multiple
898 amidated neuropeptides are required for normal circadian locomotor rhythms in
899 Drosophila. J Neurosci 21, 6673–6686. https://doi.org/10.1523/JNEUROSCI.21-17-
900 06673.2001
901 Thompson, S.N., 2003. Trehalose – The Insect 'Blood' Sugar. Advances in Insect Physiology
902 31, 205–285. https://doi.org/10.1016/S0065-2806(03)31004-5
903 van den Pol, A.N., 2012. Neuropeptide transmission in brain circuits. Neuron 76, 98–115.
904 https://doi.org/10.1016/j.neuron.2012.09.014
905 van Schaftingen, E., Gerin, I., 2002. The glucose-6-phosphatase system. Biochem J 362, 513–
906 532. https://doi.org/10.1042/0264-6021:3620513
907 Veiga-da-Cunha, M., Chevalier, N., Stephenne, X., Defour, J.-P., Paczia, N., Ferster, A.,
908 Achouri, Y., Dewulf, J.P., Linster, C.L., Bommer, G.T., Van Schaftingen, E., 2019.
909 Failure to eliminate a phosphorylated glucose analog leads to neutropenia in
910 patients with G6PT and G6PC3 deficiency. Proc Natl Acad Sci U S A 116, 1241–1250.
911 https://doi.org/10.1073/pnas.1816143116
912 Verleyen, P., Baggerman, G., Wiehart, U., Schoeters, E., Van Lommel, A., De Loof, A.,
913 Schoofs, L., 2004. Expression of a novel neuropeptide, NVGTLARDFQLPIPNamide, in
914 the larval and adult brain of Drosophila melanogaster. J Neurochem 88, 311–319.
915 https://doi.org/10.1046/j.1471-4159.2003.02161.x
916 Volkenhoff, A., Weiler, A., Letzel, M., Stehling, M., Klämbt, C., Schirmeier, S., 2015. Glial
917 Glycolysis Is Essential for Neuronal Survival in Drosophila. Cell Metab 22, 437–447.
918 https://doi.org/10.1016/j.cmet.2015.07.006
919 Wu, Q., Wen, T., Lee, G., Park, J.H., Cai, H.N., Shen, P., 2003. Developmental control of
920 foraging and social behavior by the Drosophila neuropeptide Y-like system. Neuron
921 39, 147–161. https://doi.org/10.1016/s0896-6273(03)00396-9
922 Zhao, X., Karpac, J., 2017. Muscle Directs Diurnal Energy Homeostasis through a Myokine-
923 Dependent Hormone Module in Drosophila. Curr Biol 27, 1941-1955.e6.
924 https://doi.org/10.1016/j.cub.2017.06.004
925 Zhao, X., Li, X., Shi, X., Karpac, J., 2020. Diet-MEF2 interactions shape lipid droplet
926 diversification in muscle to influence Drosophila lifespan. Aging Cell 19, e13172.
927 https://doi.org/10.1111/acel.13172
928 Zhou, W., Chang, J., Wang, X., Savelieff, M.G., Zhao, Y., Ke, S., Ye, B., 2014. GM130 is
929 required for compartmental organization of dendritic golgi outposts. Curr Biol 24,
930 1227–1233. https://doi.org/10.1016/j.cub.2014.04.008
931

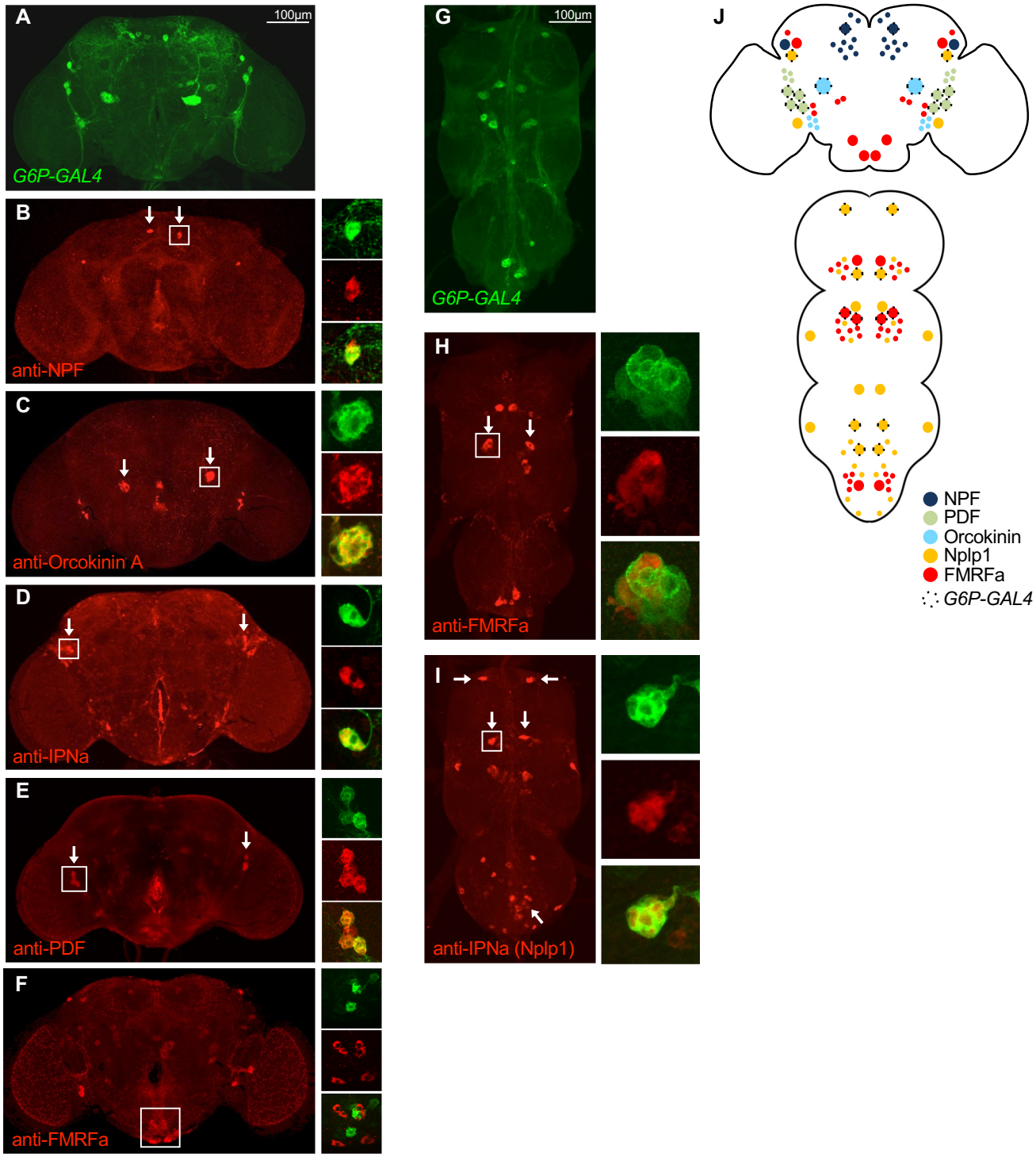
A
100µm
G6P-GAL4
B
anti-NPF
C
anti-Orcokinin A
D
anti-IPNa
E
anti-PDF
F
anti-FMRFa
G
100µm
G6P-GAL4
H
anti-FMRFa
I
anti-IPNa (Nplp1)
J
NPF
PDF
Orcokinin
Nplp1
FMRFa
G6P-GAL4

Figure 1

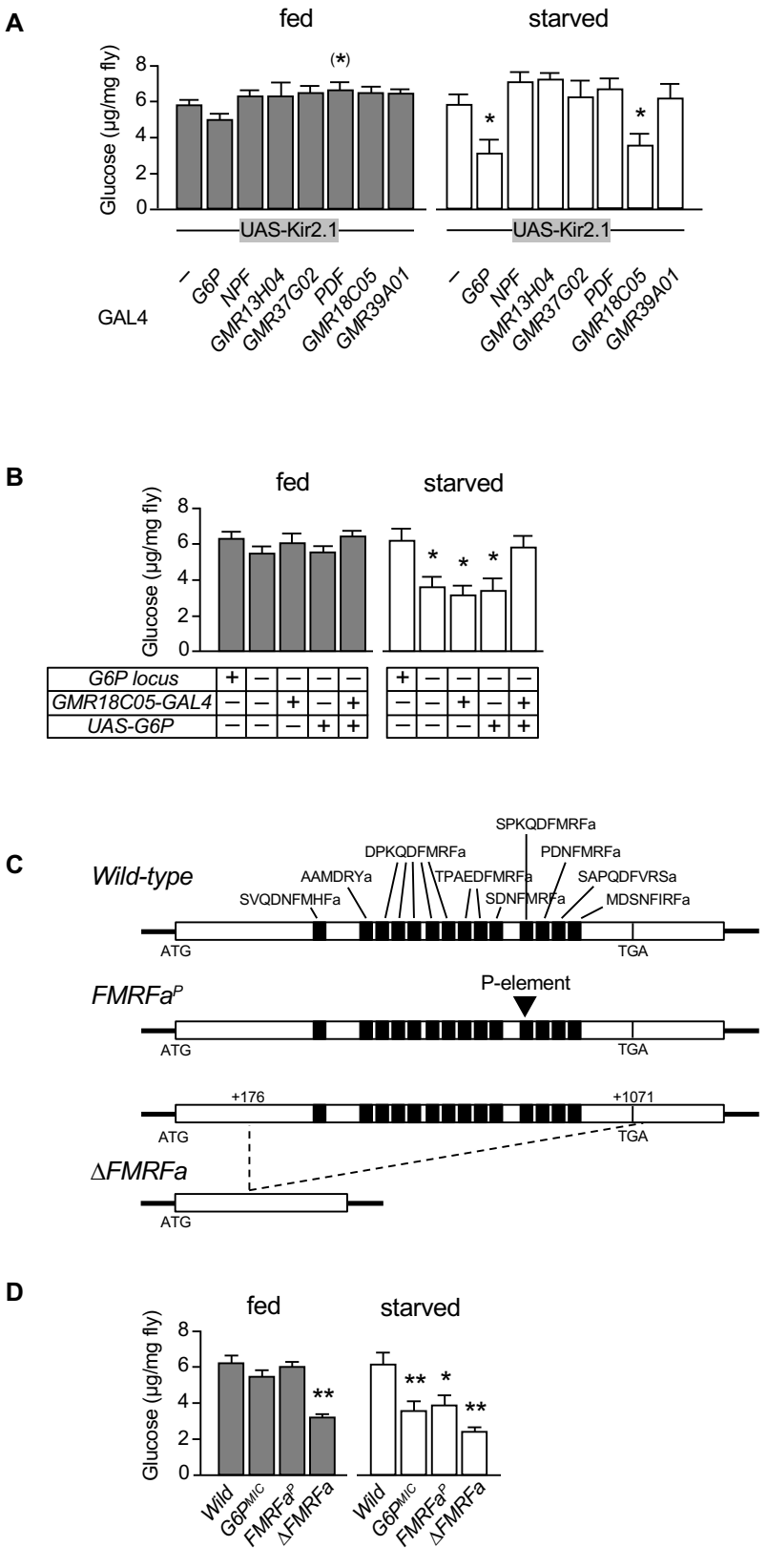
A
fed
starved
Glucose (µg/mg fly)
8
6
4
2
0
(*)
*
*
UAS-Kir2.1
UAS-Kir2.1
GAL4
/
G6P
NPF
GMR13H04
GMR37G02
PDF
GMR18C05
GMR39A01
B
fed
starved
Glucose (µg/mg fly)
G6P locus
GMR18C05-GAL4
UAS-G6P
C
Wild-type
SPKQDFMRFa
DPKQDFMRFa
PDNFMRFa
AAMDRYa
TPAEDFMRFa
SAPQDFVRSa
SVQDNFMHFa
SDNFMRFa
MDSNFIRFa
ATG
TGA
FMRFa^P
P-element
+176
+1071
ΔFMRFa
D
fed
starved
Glucose (µg/mg fly)
**
**
*
**
Wild
G6P^MIC
FMRFa^P
ΔFMRFa

Figure 2

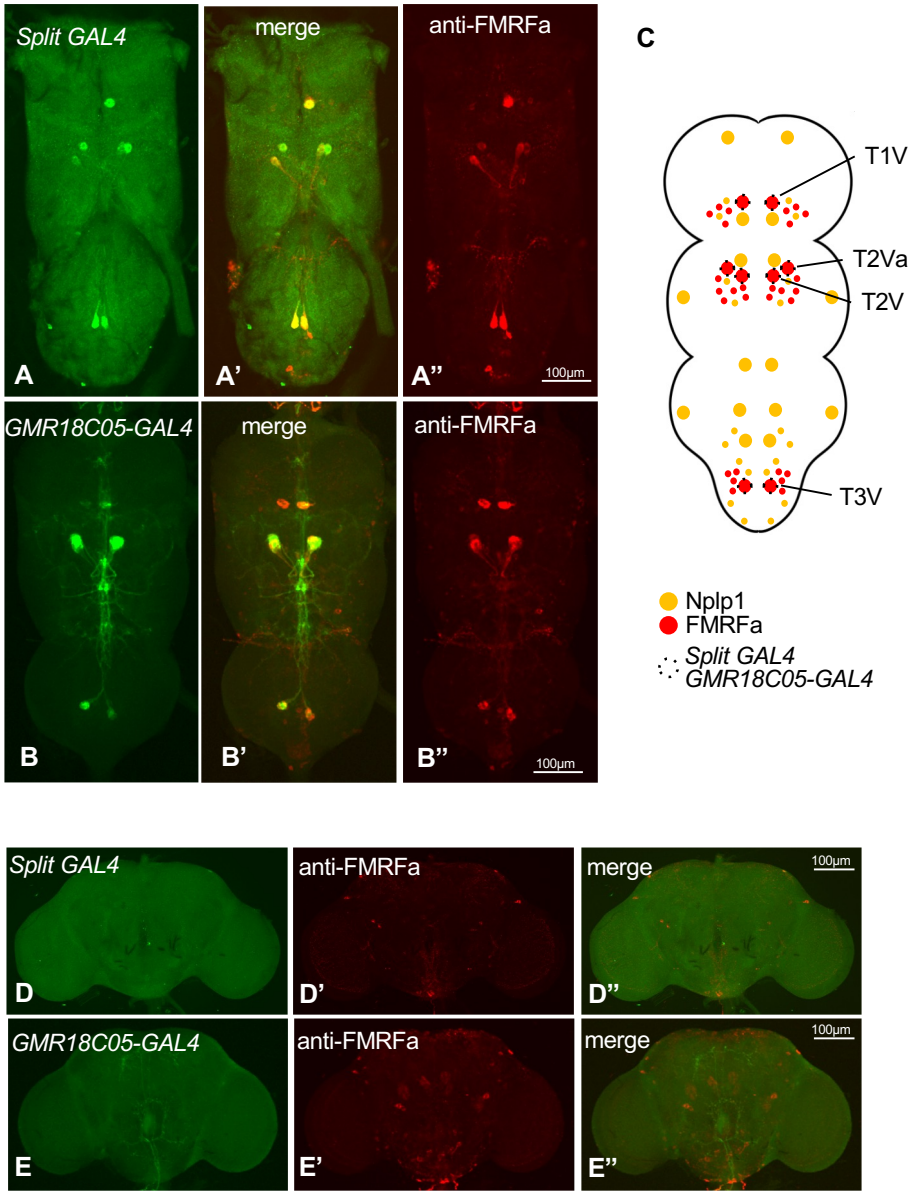
Split GAL4
merge
anti-FMRFa
A
A'
A''
100µm
GMR18C05-GAL4
merge
anti-FMRFa
B
B'
B''
100µm
C
T1V
T2Va
T2V
T3V
Nplp1
FMRFa
Split GAL4
GMR18C05-GAL4
Split GAL4
anti-FMRFa
merge
100µm
D
D'
D''
GMR18C05-GAL4
anti-FMRFa
merge
100µm
E
E'
E''

Figure 3

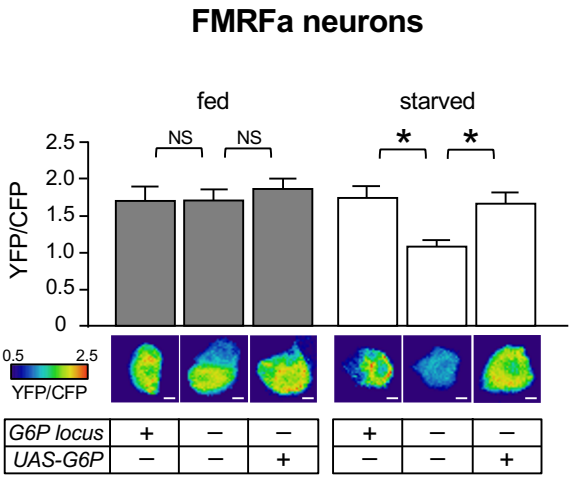
FMRFa neurons
fed
starved
NS
NS
*
*
YFP/CFP
2.5
2.0
1.5
1.0
0.5
0
0.5
2.5
YFP/CFP
G6P locus
UAS-G6P
+
−
−
−
−
+
+
−
−
−
−
+

Figure 4

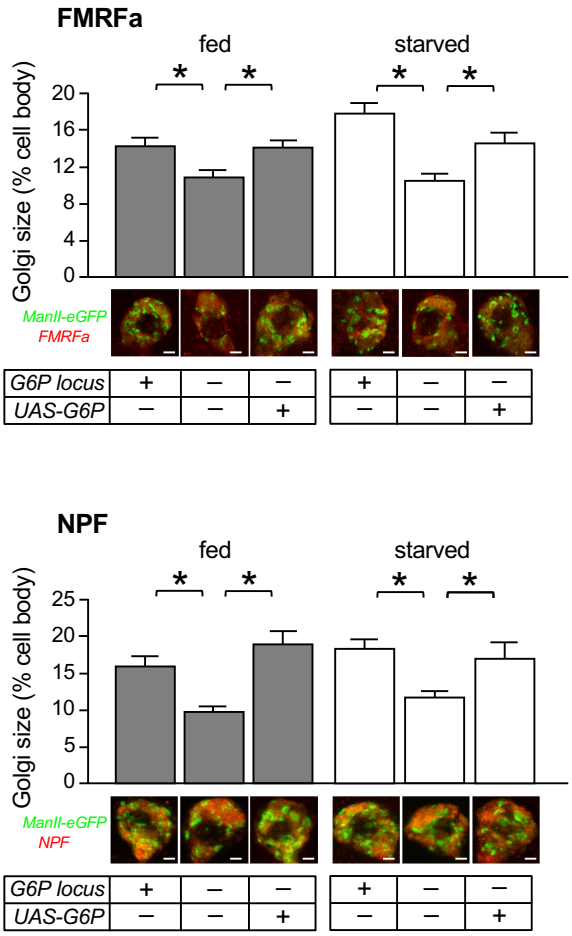
A
FMRFa
fed
starved
Golgi size (% cell body)
20
16
12
8
4
0
ManII-eGFP
FMRFa
G6P locus
UAS-G6P
B
NPF
fed
starved
Golgi size (% cell body)
25
20
15
10
5
0
ManII-eGFP
NPF
G6P locus
UAS-G6P

Figure 5

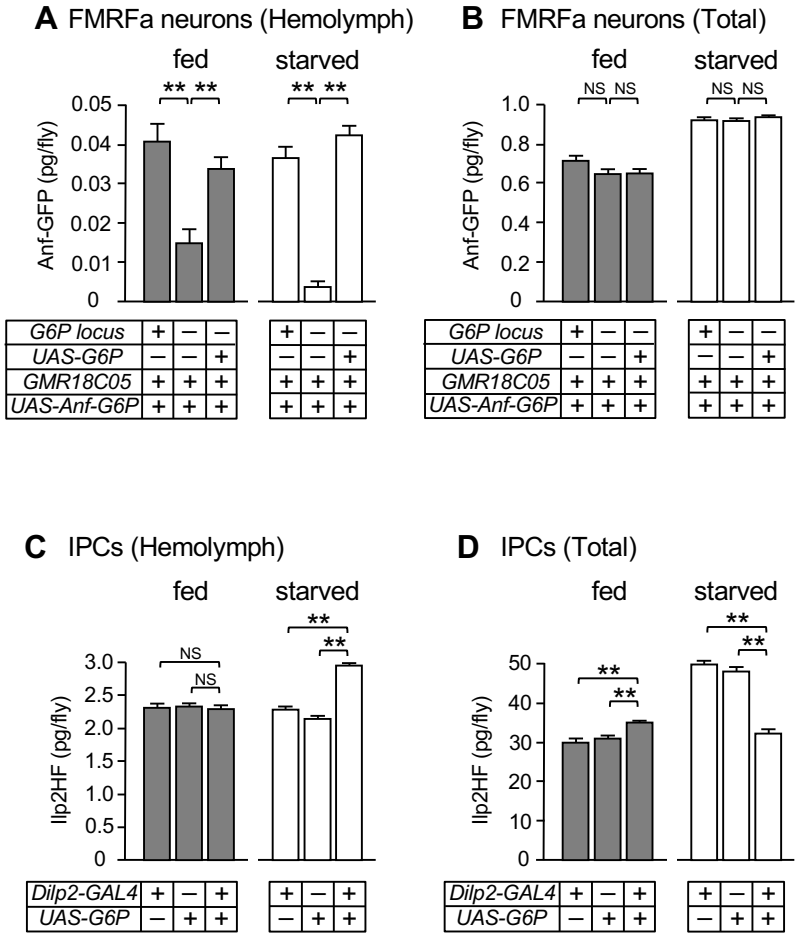
A FMRFa neurons (Hemolymph)
fed
starved
Anf-GFP (pg/fly)
0.05
0.04
0.03
0.02
0.01
0
** **
** **
G6P locus
UAS-G6P
GMR18C05
UAS-Anf-G6P
B FMRFa neurons (Total)
fed
starved
Anf-GFP (pg/fly)
1.0
0.8
0.6
0.4
0.2
0
NS NS
NS NS
G6P locus
UAS-G6P
GMR18C05
UAS-Anf-G6P
C IPCs (Hemolymph)
fed
starved
Ilp2HF (pg/fly)
3.0
2.5
2.0
1.5
1.0
0.5
0
NS
NS
**
**
Dilp2-GAL4
UAS-G6P
D IPCs (Total)
fed
starved
Ilp2HF (pg/fly)
50
40
30
20
10
0
**
**
**
**
Dilp2-GAL4
UAS-G6P

Figure 6

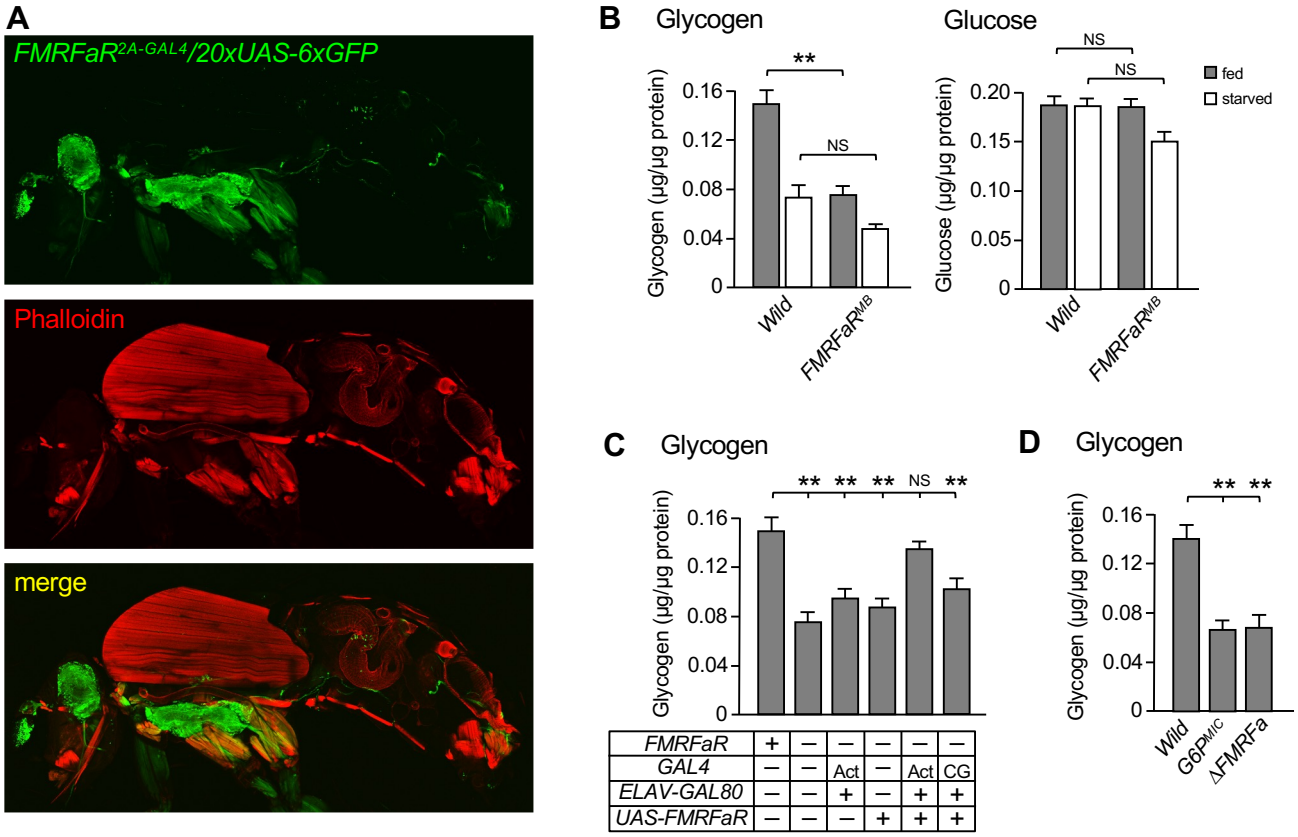
A
FMRFaR2A-GAL4/20xUAS-6xGFP
Phalloidin
merge
B
Glycogen
Glucose
Glycogen (µg/µg protein)
Glucose (µg/µg protein)
0.16
0.12
0.08
0.04
0
0.20
0.15
0.10
0.05
**
NS
fed
starved
Wild
FMRFaRMB
C
Glycogen
Glycogen (µg/µg protein)
FMRFaR + – – – – –
GAL4 – – Act – Act CG
ELAV-GAL80 – – + – + +
UAS-FMRFaR – – – + + +
D
Glycogen
Glycogen (µg/µg protein)
Wild
G6PMIC
ΔFMRFa

Figure 7